European Journal of Medicinal Chemistry 75 (2014) 31–42

Contents lists available at ScienceDirect

European Journal of Medicinal Chemistry

journal homepage: http://www.elsevier.com/locate/ejmech

Original article

Toward new classes of potent antibiotics: Synthesis and antimicrobial activity of novel metallosaldach–imidazolium salts

Reda F.M. Elshaarawy [a, b, *], Christoph Janiak [b, **]

[a] Faculty of Science, Suez University, Suez, Egypt
[b] Institut für Anorganische Chemie und Strukturchemie, Heinrich-Heine Universität Düsseldorf, 40204 Düsseldorf, Germany

ARTICLE INFO

Article history:
Received 16 May 2013
Received in revised form
17 July 2013
Accepted 9 September 2013
Available online 19 September 2013

Keywords:
N,N′-Bis(salicylidene)-1,2-diaminocyclohexane
Imidazolium chlorides
Complexes
Spectral study
Antimicrobial survey

ABSTRACT

Imidazolium salts (Im^{+}–R^2R^3–Cl^{-}) attached to the *N,N′*-bis(salicylidene)-(±)-*trans*-1,2-diaminocyclohexane (saldach) backbone (**4a**–**f**) have been designed and successfully applied for the synthesis of the corresponding mononuclear complexes with Mn(III) and Fe(III) ions. The molecular structures of the saldach ligands $H_2(R^1)_2$saldach(Im^{+}–R^2R^3–Cl^{-})$_2$ (R^1 = H, *tert*-Bu, R^2 = H, Et, *n*-Bu, R^3 = H, Me) and their [M(III)Cl{$(R^1)_2$saldach(Im^{+}–R^2R^3–Cl^{-})$_2$}] (M = Mn, Fe) complexes have been established. The free ligands exist as the phenol-OH and not as the zwitterionic (imine)N–$H^{+}\cdots{}^{-}$O(phenol) tautomer. Antimicrobial activity of the target compounds revealed higher potent antibacterial activity against *Salmonella aureus*, *B. subtilis* while less effective against *E. coli* and *C. albicans* and inactivity against *A. flavus*. Compound (**4d**) and its Fe(III) complex (**6d**) exhibit remarkable extra-potent bactericidal activity.

1. Introduction

Antibiotics have revolutionized the medical care in the 20th century. With the discovery of antibiotics, people were convinced that infectious diseases might someday be wiped out. However, the emergence and spread of multidrug-resistant bacteria have made treatment of infectious diseases difficult and have become a serious medical problem [1,2]. For example, strains of *Salmonella enterica*, a leading cause of bacterial gastroenteritis, are no longer susceptible to front line antibiotics [3] and the distribution of methicillin-resistant *Salmonella aureus* (MRSA) strains has increased [4]. Moreover, the high level of inherent antibiotic resistance in *P. aeruginosa* makes treatment of these infections problematic [5]. This has given urgency to research to develop a variety of interesting compounds as drugs used in many fields. Several approaches for negating antibiotic resistance are currently being investigated, including inactivation of enzymes in essential metabolic pathways and inhibiting signal transduction systems [6,7]. These approaches involve the development of new antimicrobial drugs with modes of action that circumvent current resistance mechanisms [8,9].

Notably, the salen type compounds prepared by the condensation of *o*-hydroxyaldehydes and diamine such as 1,2-diaminocyclohexane (DACH, dach) present versatile steric, electronic and liphophilic properties [10]. Salen type compounds have tremendous potential for a host of pharmaceutical applications; their enormous effects on different models have raised serious possibilities recently for their use as starting materials in the synthesis of antibiotics, antiallergic, antiphlogistic and antitumor drugs [11–13]. Unparalleled attention has been devoted to these materials due to their low cost, ease of fabrication and their stability. A tautomeric equilibrium has been recognized in 2-hydroxy Schiff bases due to the existence of (phenol)O–H$^{\cdots}$N(imine) and (phenol)$O^{-\cdots+}$H–N(imine) type hydrogen bonds. This equilibrium can be shifted to the zwitterionic form due to external electric fields from additional ionic charges within the molecule and molecular packing (Scheme 1) [14]. Hydrogen bonding interactions play roles in preferential solvation and have been investigated because they are present in a large variety of chemical, biochemical and pharmacological events. In salen compounds, the imine nitrogen can acts as intramolecular hydrogen bond acceptor and the phenolic oxygen derivatives can act as intermolecular hydrogen bond acceptor. Moreover, the conjugation between metal ions and biologically active Schiff bases becomes a subject worthy of pursuit

* Corresponding author. Faculty of Science, Suez University, Suez, Egypt.
** Corresponding author.
E-mail addresses: reda_elshaarawi@science.suez.edu.eg, Reda.El-Shaarawy@uni-duesseldorf.de, reda_shaarauy@yahoo.com (R.F.M. Elshaarawy), janiak@uni-duesseldorf.de (C. Janiak).

0223-5234/$ – see front matter © 2014 Elsevier Masson SAS. All rights reserved.
http://dx.doi.org/10.1016/j.ejmech.2013.09.029

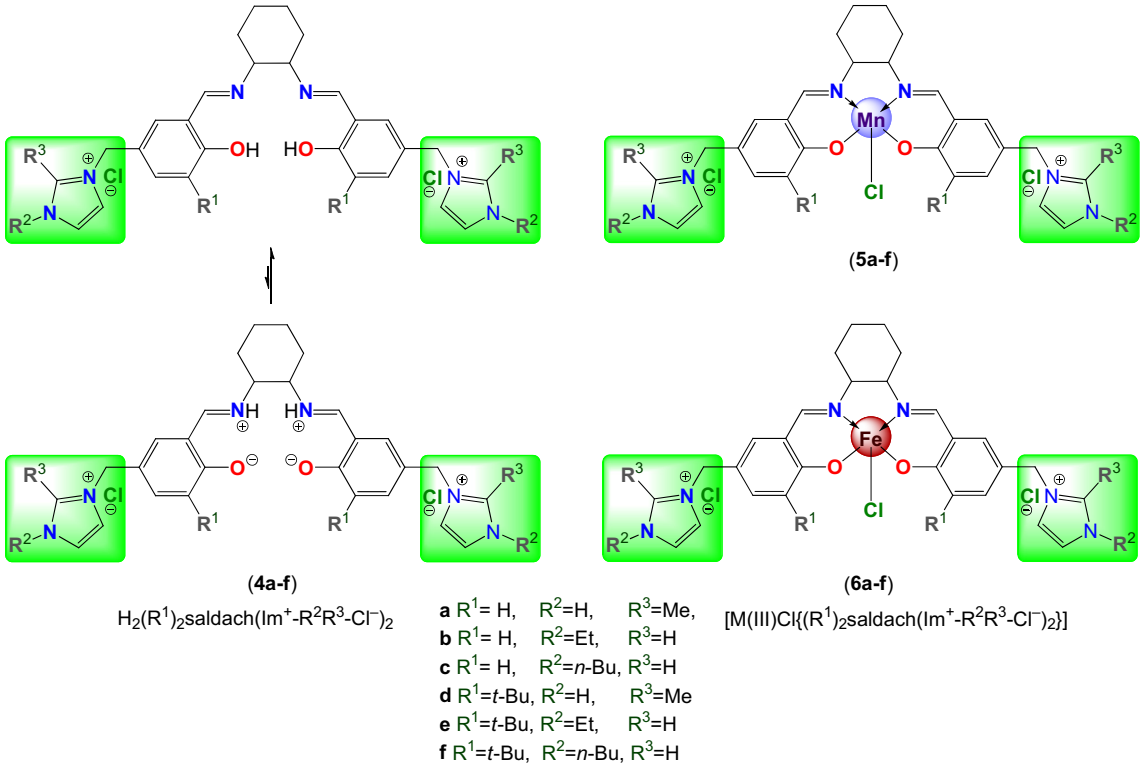

Scheme 1. Saldach–imidazolium chloride ligands with the tautomeric equilibrium and Mn(III)- and Fe(III)-saldach–imidazolium chloride complexes used in this work.

and has demonstrated great promise for their extensive applications in the enhancement of their biological and biomedical activities [13,15–17].

At the same time, salt formation of Active Pharmaceutical Ingredients (APIs) is an attractive and commonly used approach to overcome the problems of solubility and stability of APIs. There are many well-known examples where biological active cations and anions combine together and the resulted salt exhibits the therapeutic effects of both of its components [18]. Therefore, it is quite reasonable to think that imidazolium salt units (as common in ionic liquids (ILs)) could potentially be included in anti-cancer, anti-viral and other therapeutic agents/drugs. These 'therapeutic ionic salts' offer distinctly different properties than the non-ionic backbone. If there is a therapeutic response then the major advantage of ionic salts would be in managing/tuning their toxicity while tailoring the physiochemical and pharmacological properties necessary for desired therapeutic applications. Recently the *in vitro* antimicrobial, biodegradability [19] and anti-tumor activities [20] of a series of imidazolium based ionic liquids were reported. The imidazolium salts examined exhibit broad activities against *cocci*, *rods* and *fungi*. Also the structure–activity relationship showed that chain length of *N*-3 alkyl substitution plays a significant role in the anti-tumor activity and cytotoxicity.

In a continuation of our earlier endeavor [21] to design and synthesize novel bioactive compounds, the present work reports the synthesis and characterization of new saldach-imidazolium salts (ionic compounds) and their metal complexes (Scheme 1). In view of the already known independent biological importance of metallosaldach compounds and imidazolium ILs, we also explore here the *in vitro* antimicrobial activity of Mn(III)- and Fe(III) saldach–imidazolium salt systems (Scheme 1) against two Gram-positive, two Gram-negative bacteria and two different fungi. These ionic salts may promise potential therapeutics to combat antibiotic resistance. Herein, Mn(III) and Fe(III) species have been chosen in this study due to their potential importance and useful applications in the biological field.

2. Experimental section

2.1. Physical measurements

Elemental analyses for C, H, N, were performed with a Perkin–Elmer 263 elemental analyzer. FT-IR spectra were recorded on a BRUKER Tensor-37 FT-IR spectrophotometer in the range 400–4000 cm^{-1} as KBr discs or in the 4000–550 cm^{-1} region with 2 cm^{-1} resolution with an ATR (attenuated total reflection) unit (Platinum ATR-QL, Diamond). For signal intensities the following abbreviations were used: br (broad), sh (sharp), w (weak), m (medium), s (strong), vs (very strong). UV/Vis spectra were measured at 25 °C in deionized water (H_2O) (10^{-5} mol/L) on a Shimadzu UV-2450 spectrophotometer using quartz cuvettes (1 cm). NMR-spectra were obtained with a Bruker Avance DRX200 (200 MHz for ^1H) or Bruker Avance DRX500 (500 MHz for ^{13}C) spectrometer with calibration to the residual proton solvent signal in DMSO-d_6 (^1H NMR: 2.52 ppm, ^{13}C NMR: 39.5 ppm), $CDCl_3$ (^1H NMR: 7.26 ppm, ^{13}C NMR: 77.16 ppm) against TMS with $\delta = 0.00$ ppm. Multiplicities of the signals were specified s (singlet), d (doublet), t (triplet), q (quartet) or m (multiplet). The mass spectra of the synthesized sal–imidazolium, saldach–imidazolium chlorides and their complexes were acquired in the linear mode for positive ions on a Bruker Ultraflex MALDI-TOF instrument equipped with a 337 nm nitrogen laser pulsing at a repetition rate of 10 Hz. The MALDI matrix material (1,8-dihydroxy-9(10H)-anthracenone (dithranol, DIT) ($C_{14}H_{10}O_3$, $M = 226.23$)) was dissolved in chloroform at a concentration of 10 mg/mL. MALDI probes were prepared by mixing compound solutions (1 mg/mL in CH_2Cl_2) with the

matrix solution (1:10, v/v) in a 0.5 mL Eppendorf® micro tube. Finally 0.5 μL of this mixture was deposited on the sample plate dried at room temperature and then analyzed. The molar conductance 10^{-3} M solution of various salts has been measured at ambient temperature with a digital conductivity meter (S30 SevenEasy™ conductivity, Mettler-Toledo Electronics, LLC, Polaris Parkway, Columbus). The overall accuracy of the conductance measurements was found to be ±0.2%. Magnetic measurements of target complexes were carried out at room temperature using a Vibrating Sample Magnetometer (VSM), (Model PAR 155).

2.2. Materials and syntheses

Chemicals were obtained from the following suppliers and used without further purification: salicylaldehyde (sal), 2-*tert*-butylphenol (2-^{t}BuPhOH), 1-ethylimidazole (1-Et-Im), 2-methylimidazole (2-Me-Im), (±)-trans-1,2-diaminocyclohexane (dach), tetrabutyl-ammonium bromide (^{t}Bu$_4$NBr), anhydrous magnesium dichloride ($MgCl_2$) and manganese(II) acetate tetrahydrate ($Mn(CH_3COO)_2 \cdot 4H_2O$) (Sigma–Aldrich), paraformaldehyde ($(CH_2O)_n$) (Roth), 1-butylimidazole (1-^{n}Bu-Im) (Alfa Aesar), triethyl amine (Et_3N) and anhydrous zinc chloride ($ZnCl_2$) (Grüssing GmbH) and iron(III) chloride hexahydrate ($FeCl_3 6H_2O$) (Acros). 3-*tert*-Butyl-2-hydroxybenzaldehyde (**1b**) was synthesized from 2-*tert*-butylphenol as described previously [22] and obtained as a pale yellow oil (82% yield). It becomes dark green on storage. ^{1}H NMR (200 MHz, $CDCl_3$) δ (ppm): 11.87 (s, 1H, Ph-O**H**), 9.91 (s, 1H, **H**C=O), 7.58 (dd, 1H, J_{HH} = 1.66, 6.02 Hz, Ph-**H**), 7.44 (dd, 1H, J_{HH} = 1.69, 7.67 Hz, Ph-**H**), 6.99 (t, 1H, J_{HH} = 7.68 Hz, Ph-**H**), 1.48 (s, 9H, C(C**H$_3$**)$_3$).

2.2.1. 5-Chloromethyl-2-hydroxybenzaldehyde (**2a**)

This compound was synthesized from salicylaldehyde according to the classical chloromethylation procedure [23] modified with catalyst $ZnCl_2$, and hydrogen chloride gas atmosphere. In a typical synthesis, 17.5 g (160 mmol) of salicylaldehyde was treated with 24 ml of 37% aqueous formaldehyde and 1.2 g (8.8 mmol) of $ZnCl_2$ in 100 ml of concentrated hydrochloric acid. The mixture was stirred at room temperature under HCl_g atmosphere (HCl_g was generated in another system, connected to the reaction vessel, by dropping concentrated H_2SO_4 slowly onto solid NaCl) for 24 h. The white solid that separated from the reaction mixture was filtered, redissolved in diethyl ether, and the combined organic phases were washed several times with milli-Q water, till pH = 7 for washing liquor, and then dried over sodium sulfate. Volatiles were distilled off under inert atmosphere, and the resulting white crude residue was filtered and further recrystallized from *n*-hexane to furnish 5-chloromethyl-2-hydroxybenzaldehyde as white-colored needles (15.2 g, 62.0% yield). FT-IR (ATR, cm^{-1}): 3240 (m, br, ν OH), 3120 (m, br, ν_{asym} CH, Ph), 3050 (m, br, ν_{sym} CH, Ph), 2876 (m, sh, ν CH_2), 1659 (vs, sh, ν C=O), 1578, 1489, 1437 (s, sh, ν C=C_{arom} + ν C–H bend), 1338 (m, sh, ν CH_2), 1252 (s, sh, ν CH_2Cl), 1150 (s, sh, ν HCC, Ph), 772 (s, sh, ν C–Cl). ^{1}H NMR (200 MHz, $CDCl_3$) δ (ppm): 11.07 (s, 1H, Ph-O**H**) 9.90 (s, 1H, Ph-**H**C=O), 7.59–7.55 (m, 2H, 2× Ph-**H**), 7.02–6.98 (d, 1H, J_{HH} = 8.34 Hz, Ph-**H**), 4.60 (s, 2H, C**H$_2$**-Ph). ^{13}C NMR (500 MHz, $CDCl_3$) δ (ppm): 196.02 (H**C**=O), 160.90 (**C**–OH), 137.22 (**C**, Ph), 133.64 (**C**H, Ph), 129.86 (**C**H, Ph), 120.34 (**C**, Ph), 118.72 (**C**H, Ph), 45.28 **C**H_2-phenyl).

2.2.2. 3-tert-Butyl-5-chloromethyl-2-hydroxybenzaldehyde (**2b**)

A mixture of **1b** (2.7 g, 15.2 mmol), $(CH_2O)_n$ (1.0 g, 33.3 mmol), and ^{t}Bu$_4$NBr (0.47 g, 1.46 mmol) in 11 ml of concentrated hydrochloric acid was stirred vigorously at ambient temperature for 72 h [24]. The resulting emulsion was extracted with diethyl ether (3 × 25 mL). Then the organic phase was washed with saturated brine solution (2 × 10 ml), milli-Q water (5 × 10 ml) and, then dried over anhydrous magnesium sulfate. This extract was further concentrated under vacuum to give 3-*tert*-butyl-5-(chloromethyl)-2-hydroxybenzaldehyde **2b** as a pale yellow crystalline solid (1.99 g, 58% yield). FT-IR (ATR, cm^{-1}): 3428 (m, br, ν OH), 3154 (m, br, ν_{asym} CH, Ph), 3070 (m, br, ν_{sym} CH, Ph), 2956 (m, sh, ν CH_3), 2848 (m, sh, ν CH_2), 1651 (vs, sh, ν C=O), 1612, 1476, 1435 (s, sh, ν C=C_{arom} + ν C–H bend), 1331 (m, sh, ν CH_2), 1263 (s, sh, ν CH_2Cl), 1172 (s, sh, ν HCC, Ph), 694 (s, sh, C–Cl). ^{1}H NMR (200 MHz, $CDCl_3$) δ (ppm): 11.90 (s, 1H, Ph-O**H**) 9.91 (s, 1H, Ph-**H**C=O), 7.57–7.56 (d, H, J_{HH} = 2.29, Ph-**H**), 7.47–7.46 (d, 1H, J_{HH} = 2.27, Ph-**H**), 4.63 (s, 2H, C**H$_2$**-Ph), 1.46 (s, 9H, C(C**H$_3$**)$_3$). ^{13}C NMR (500 MHz, $CDCl_3$) δ (ppm): 192.98 (H**C**=O), 160.27 (**C**–OH), 136.88 (**C**, Ph), 133.78 (**C**H, Ph), 130.36 (**C**, Ph), 129.00 (**C**, Ph), 125.17 (**C**H, Ph), 46.06 (**C**H_2-Ph), 31.89 (**C**$(CH_3)_3$), 30.56 (C(**C**H_3)$_3$).

2.2.3. Preparation of salicylaldehyde-alkylimidazolium chlorides $H(R^1)sal(Im^+–R^2R^3–Cl^-)$ (**3a–f**)

2.2.3.1. General method. To a vigorously stirred solution of imidazole derivatives (23.39 mmol) in dry toluene (10 mL) at room temperature was added the solution of chloromethyl-salicylaldehydes **2a**, **b** (19.50 mmol) in dry toluene (10 mL), drop-wise, under nitrogen atmosphere. The resulting solution was further stirred at 60 °C for 24 h. The product separated out was washed twice with toluene (2 × 5 mL) and several times with ether (5 × 10 mL), to remove the unreacted materials, and dried under vacuum to give pale yellow solid which used for the following preparations without further purification. Samples of the products were nevertheless isolated and fully characterized, as described below.

*2.2.3.2. 3-(3-Formyl-4-hydroxybenzyl)-2-methyl-1H-imidazol-3-ium chloride (**3a**).* Obtained as pale yellow solid (4.48 g, 91%). FT-IR (KBr, cm^{-1}): 3364 (m, br, ν N(1)–H and O–H), 3161 (m, br, ν_{asym} CH, CH, Im and Ph), 3080 (m, br, ν_{sym} CH, Im and Ph), 2979 (m, sh, ν_{asym} CH_3), 2959 (m, sh, ν_{sym} CH_3), 2884 (m, sh, ν CH_2), 1661 (vs, sh, ν C=O), 1573, 1485, 1455 (s, sh, ν C=C_{arom} + ν C–H bend), 1338 (m, sh, ν CH_2), 1149 (s, sh, HCC, HCN bending, Im), 823 (m, sh), 750 (m, sh), 682 (m, sh), 555 (m, sh). ^{1}H NMR (200 MHz, $CDCl_3$) δ (ppm): 10.83 (s, 1H, Ph-**H**C=O) 10.30 (s, 1H, Ph-O**H**), 10.15 (s, 1H, N–**H** Im), 7.86–7.81 (d, 1H, J_{HH} = 1.39 Hz, N(1)CHC**H**-Im), 7.76–7.74 (d, J_{HH} = 1.41 Hz, 1H, N(1)C**H**CH-Im), 7.47–7.13 (m, 3H, 3× Ph-**H**), 5.45 (s, 2H, –N(3)–C**H$_2$**-Ph), 2.57 (s, 3H, C(2)–C**H$_3$**). ^{13}C NMR (500 MHz, $CDCl_3$) δ (ppm): 196.89 (H**C**=O), 159.21 (**C**–OH), 144.8 (–N(1)**C**(CH_3)N(3)–), 136.68 (**C**–C=O), 136.47 (**C**H, Ph), 130.99 (**C**H, Ph), 127.35 (**C**, Ph), 122.74 ((–N(1)CH**C**H–), 122.41 (–N(1)**C**HCH–), 117.88 (**C**H, Ph), 51.88 (–N(1)**C**H_2-Ph), 22.73 (C(2)–**C**H_3). MALDI-TOF MS, *m/z*: 217.1 $[M - Cl]^+$.

*2.2.3.3. 1-Ethyl-3-(3-formyl-4-hydroxybenzyl)-1H-imidazol-3-ium chloride (**3b**).* Obtained as yellow solid (3.56 g, 69%). FT-IR (KBr, cm^{-1}): 3343 (m, br, ν O–H), 3135 (m, br, ν_{asym} CH, Im and Ph), 3098 (m, br, ν_{sym} CH, Im and Ph), 2933 (m, sh, ν_{asym} CH_3), 2908 (m, sh, ν_{sym} CH_3), 2843 (m, sh, ν CH_2), 1662 (vs, sh, ν C=O), 1568, 1497, 1458 (s, sh, ν C=C_{arom} + ν C–H bend), 1249 (m, sh, δ CH_3 + ν N–CH_2), 1152 (s, sh, ν HCC + ν HCN bending, Im), 825 (m, sh), 759 (m, sh), 682 (m, sh), 558 (m, sh). ^{1}H NMR (200 MHz, $CDCl_3$) δ (ppm): 10.99 (s, 1H, Ph-**H**C=O), 10.29 (s, 1H, Ph-O**H**), 9.31 (s, 1H, –N(1)C**H**N(3)-Im), 7.83–7.81 (d, J_{HH} = 1.51 Hz, 1H, N(1)CHC**H**-Im), 7.77–7.75 (d, J_{HH} = 1.60 Hz, 1H, N(1)C**H**CH-Im), 7.69 (s, 1H, Ph-H), 7.59–7.57 (d, 1H, J_{HH} = 7.02 Hz, Ph-H), 7.18–7.16 (d, 1H, J_{HH} = 8.34 Hz, Ph-H), 5.36 (s, 2H, –N(3)–C**H$_2$**-Ph), 4.16–4.12 (q, 2H, –N(1)C**H$_2$**), 1.27–1.24 (t, J_{HH} = 7.30, 7.34 Hz, 3H, –CH_2C**H$_3$**). ^{13}C NMR (500 MHz, $CDCl_3$) δ (ppm): 196.16 (H**C**=O), 158.98 (**C**–OH), 139.02 (–N(1)**C**HN(3)–), 136.17 (**C**–C=O), 136.06 (**C**H, Ph), 130.64 (**C**H, Ph), 126.89 (**C**, Ph), 123.00 ((–N(1)CH**C**H–), 122.92 (–N(1)**C**HCH–), 117.32 (**C**H, Ph), 53.68 (–N(1)**C**H_2-phenyl), 41.54 (N(1)–**C**H_2), 15.79 (CH_3, CH_2–**C**H_3). MALDI-TOF MS, *m/z*: 231.1 $[M - Cl]^+$.

*2.2.3.4. 1-Butyl-3-(3-formyl-4-hydroxybenzyl)-1H-imidazol-3-ium chloride (**3c**).* Obtained as yellow solid (4.90 g, 86%). FT-IR (KBr, cm^{-1}): 3359 (m, br, ν O–H), 3185 (m, br, ν_{asym} CH, Im and Ph), 3066 (m, br, ν_{sym} CH, Im and Ph), 2981 (m, sh, ν_{asym} CH_3), 2960 (m, sh, ν_{sym} CH_3), 2877 (m, sh, ν CH_2), 1657 (vs, sh, ν C=O), 1569, 1552, 1469 (s, sh, ν C=C_{arom} + ν C–H bend), 1336 (m, sh, δ CH_3 + δ CH_2), 1245 (m, sh, δ CH_3 + ν N–CH_2), 1149 (s, sh, ν HCC + ν HCN bending, Im), 850 (m, sh), 736 (m, sh), 679 (m, sh), 582 (m, sh). ^{1}H NMR (200 MHz, $CDCl_3$) δ (ppm): 11.37 (s, 1H, Ph-**H**C=O) 10.30 (s, 1H, Ph-O**H**), 9.53 (s, 1H, –N(1)C**H**N(3)–Im), 7.88–7.86 (d, 2H, N(1)C**H**C**H**-Im), 7.74 (s, 1H, Ph-H), 7.66–7.64 (d, 1H, J_{HH} = 6.99 Hz, Ph-H), 7.26.7.24 (d, 1H, J_{HH} = 8.56 Hz, Ph-H), 5.40 (s, 2H, –N(3)–C$\mathbf{H_2}$–Ph), 4.20–4.17 (t, J_{HH} = 7.06, 7.14 Hz, 2H, –N(1)C$\mathbf{H_2}$), 1.79–1.73 ($m_{(5)}$, 2H, –N(1)CH_2C$\mathbf{H_2}$), 1.27–1.19 ($m_{(6)}$, 2H, –C$\mathbf{H_2}$$CH_3$), 0.89–0.86 (t, J_{HH} = 7.33, 7.38 Hz, 3H, –CH_2C$\mathbf{H_3}$). ^{13}C NMR (500 MHz, $CDCl_3$) δ (ppm): 195.81 (H**C**=O), 159.04 (**C**–OH), 138.51 (–N(1)**C**HN(3)–), 136.10 (**C**–C=O), 135.89 (**C**H, Ph), 130.96 (**C**H, Ph), 126.73 (**C**, Ph), 123.23 (–N(1)CH**C**H–), 123.02 (–N(1)**C**HCH–), 116.77 (**C**H, Ph), 53.74 (–N(1)**C**H_2-phenyl), 48.13 (N(1)–**C**H_2), 34.79 (N(1)–CH_2–**C**H_2), 19.44 (–**C**H_2–CH_3), 13.40 (–CH_2–**C**H_3). MALDI-TOF MS, *m/z*: 259.2 [M – Cl]$^+$.

*2.2.3.5. 3-(3-(tert-Butyl)-5-formyl-4-hydroxybenzyl)-2-methyl-1H-imidazol-3-ium chloride (**3d**).* Obtained as faint yellow semi-solid (3.65 g, 88%). ^{1}H NMR (200 MHz, $CDCl_3$) δ (ppm): 11.91 (s, 1H, Ph-**H**C=O) 10.79 (s, 1H, Ph-O**H**), 9.91 (s, 1H, –N–**H** Im), 7.85–7.83 (d, 1H, J_{HH} = 1.60 Hz, N(1)CHC**H**-Im), 7.55–7.54 (d, J_{HH} = 1.60 Hz, 1H, N(1)C**H**CH-Im), 7.27 (s, 1H, Ph-**H**), 7.01 (s, 1H, Ph-**H**), 5.53 (s, 2H, –N(3)–C$\mathbf{H_2}$-Ph), 2.78 (s, 3H, C(2)–C$\mathbf{H_3}$), 1.38 (s, 9H, C(C$\mathbf{H_3}$)$_3$). ^{13}C NMR (500 MHz, $CDCl_3$) δ (ppm): 196.84 (H**C**=O), 160.26 (**C**–OH), 145.32 (–N(1)**C**(CH_3)N(3)–), 135.48 (**C**–C(CH_3)$_3$), 133.88 (**C**H, Ph), 129.06 (**C**, **C**–C=O), 127.24 (**C**H, Ph), 124.6 (**C**, Ph), 123.45 ((–N(1) CH**C**H–), 122.93 (–N(1)**C**HCH–), 52.00 (–N(1)CH_2-Ph), 34.41 (C–**C**(CH_3)$_3$), 29.97 (C–C(**C**H_3)$_3$), 18.52 (C(2)–**C**H_3), MALDI-TOF MS, *m/z*: 273.1 [M – Cl]$^+$.

*2.2.3.6. 3-(3-(tert-Butyl)-5-formyl-4-hydroxybenzyl)-1-ethyl-1H-imidazol-3-ium chloride (**3e**).* Obtained as yellow-orange wax (2.98 g, 58%). ^{1}H NMR (200 MHz, $CDCl_3$) δ (ppm): 11.93 (s, 1H, Ph-**H**C = O) 9.98 (s, 1H, Ph-O**H**), 9.91 (s, 1H, –N(1)C**H**N(3)-Im), 7.86–7.84 (d, 1H, J_{HH} = 1.59 Hz, N(1)CHC**H**-Im), 7.56–7.54 (d, J_{HH} = 1.63 Hz, 1H, N(1)C**H**CH-Im), 7.34 (s, 1H, Ph-**H**), 7.26 (s, 1H, Ph-**H**), 5.52 (s, 2H, –N(3)–C$\mathbf{H_2}$-Ph), 4.22–4.11 (q, 2H, –N(1)C$\mathbf{H_2}$), 1.39 (s, 9H, C(C$\mathbf{H_3}$)$_3$), 1.26–1.20 (t, J_{HH} = 7.28, 7.30 Hz, 3H, –CH_2C$\mathbf{H_3}$). ^{13}C NMR (500 MHz, $CDCl_3$) δ (ppm): 196.89 (H**C**=O), 155.73 (**C**–OH), 137.69 (**C**, Ph), 135.81 (–N(1)**C**HN(3)–), 133.23 (**C**H, Ph), 130.33 (**C**, **C**–C=O), 128.57 (**C**, Ph), 125.06(**C**H, Ph), 123.43 (–N(1)CH**C**H–), 122.02 (–N(1)**C**HCH–), 54.74 (–N(3)**C**H_2–Ph), 41.13 (N(1)–**C**H_2), 34.40 (**C**(CH_3)$_3$), 29.33 (C(**C**H_3)$_3$), 16.08 (CH_2**C**H_3). MALDI-TOF MS, *m/z*: 287.2 [M – Cl]$^+$.

*2.2.3.7. 3-(3-(tert-Butyl)-5-formyl-4-hydroxybenzyl)-1-butyl-1H-imidazol-3-ium chloride (**3f**).* Obtained as yellow solid (3.88 g, 77%). FT-IR (KBr, cm^{-1}): 3465 (m, br, ν O–H), 3101 (m, br, ν_{sym} CH, Im and Ph), 2976 (m, sh, ν_{asym} CH_3), 2942 (m, sh, ν_{sym} CH_3), 2883 (m, sh, ν CH_2), 1650 (vs, sh, ν C=O), 1541, 1477, 1445 (s, sh, ν C=C_{arom} + ν C–H bend), 1333 (m, sh, ν CH_2), 1162 (s, sh, HCC, HCN bending, Im), 851 (m, sh), 749 (m, sh), 679 (m, sh), 558 (m, sh). ^{1}H NMR (200 MHz, $CDCl_3$) δ (ppm): 11.88 (s, 1H, Ph-**H**C = O) 10.11 (s, 1H, Ph-O**H**), 9.83 (s, 1H, –N(1)C**H**N(3)-Im), 7.87–7.86 (d, 2H, N(1)C**H**C**H**-Im), 7.60–7.57 (d, 1H, J_{HH} = 7.01 Hz, Ph-**H**), 7.25–7.21 (d, 1H, J_{HH} = 8.55 Hz, Ph-**H**), 5.49 (s, 2H, –N(3)–C$\mathbf{H_2}$-Ph), 4.09–3.97 (t, J_{HH} = 7.02, 6.99 Hz, 2H, –N(1)C$\mathbf{H_2}$), 1.69–1.65 ($m_{(5)}$, 2H, –N(1)CH_2C$\mathbf{H_2}$), 1.31 (s, 9H, C(C$\mathbf{H_3}$)$_3$), 1.28–1.20 ($m_{(6)}$, 2H, –C$\mathbf{H_2}$$CH_3$), 0.92–0.89 (t, J_{HH} = 7.18, 7.17 Hz, 3H, –CH_2C$\mathbf{H_3}$). MALDI-TOF MS, *m/z*: 315.2 [M – Cl]$^+$.

*2.2.4. General procedure for the preparation of salen ligands $H_2(R^1)_2$saldach(Im^+–R^2R^3–Cl^-)$_2$ (**4a–f**)*

A methanolic solution (10 mL) of (±)-*trans*-1,2-diaminocyclohexane (dach) (0.23 g, 2.0 mmol), in a Schlenk tube, was added drop-wise to a methanolic solution (20 mL) of substituted salicylaldehyde-imidazolium salt H(R^1)sal(Im^+–R^2R^3–Cl^-) **3a–f** (4.0 mmol) into a 100 ml Schlenk flask under nitrogen atmosphere. The reaction mixture was stirred at 60 °C overnight. MeOH was partially removed under reduced pressure on a rotary evaporator, and the yellow products of **4a–f** were precipitated by ethyl acetate and kept in the refrigerator overnight. The precipitate was sonicated with Et_2O (3 × 25 mL), collected by filtration and dried under vacuum.

*2.2.4.1. N,N′-Bis[5-((2-methylimidazolium)methylene)-salicylidene)-trans-1,2-cyclohexanediamine dichloride (**4a**).* Yellow-orange powder, (2.16 g, 87%). FT-IR (KBr, cm^{-1}): 3395 (m, br, ν N(1)–H + ν O–H), 3186 (w, br, ν_{asym} CH, CH, Im and Ph), 3090 (m, br, ν_{sym} CH, Im and Ph), 2941 (m, sh, ν CH_3), 2861 (m, sh, ν CH_2), 1630 (vs, sh, ν C=N), 1558, 1475, 1443 (s, sh, ν C=C_{arom} + ν C–H bend), 1320 (m, sh, ν CH_2), 1258 (m, sh, ν Ph-O), 1160 (s, sh, ν HCC + ν HCN bending, Im). ^{1}H NMR (200 MHz, $CDCl_3$) δ (ppm): 13.30 (br, s, 2H, Ph-O**H**), 9.48 (s, 2H, Im-N**H**), 8.62 (s, 2H, 2× **H**–C=N), 7.86–7.84 (d, 2H, J_{HH} = 1.76 Hz, 2× N(1)CHC**H**-Im), 7.63–7.62 (d, J_{HH} = 2.02 Hz, 2H, 2× N(1)C**H**CH-Im), 7.58–7.42 (m, 4H, 4× Ph-**H**), 6.92–6.84 (m, 2H, 2× Ph-**H**), 5.30 (s, 4H, 2× –N(3)–C$\mathbf{H_2}$-Ph), 3.95-3.83 (m, 2H, 2× Cyhex-**H**), 3.38 (s, 6H, 2× Im-C$\mathbf{H_3}$), 1.79–1.42 (m, 8H, 8× Cyhex-**H**). MALDI-TOF MS, *m/z*: 659.4 [M·2H_2O + K]$^+$; HRMS (ESI): *m/z*: calcd for $C_{30}H_{36}N_6O_2$·2H_2O: 547.3835 [M·2H_2O–2Cl]$^+$; found: 547.3745. Anal. Calcd. for $C_{30}H_{36}Cl_2N_6O_2$·2H_2O (*M* = 619.58): C, 58.16; H, 6.51; N, 13.56; Found: C, 57.84; H, 6.23; N, 13.51. Conductivity = 284 μS/cm.

*2.2.4.2. N,N′-Bis[5-((1-ethylimidazolium)methylene)-salicylidene)-trans-1,2-cyclohexanediamine dichloride (**4b**).* Yellow powder, (2.51 g, 81%). FT-IR (KBr, cm^{-1}): 3434 (s, br, ν O–H), 3133 (w, br, ν_{asym} CH, CH, Im and Ph), 3068 (m, br, ν_{sym} CH, Im and Ph), 2933 (m, sh, ν CH_3), 2858 (m, sh, ν CH_2), 1632 (vs, sh, ν C=N), 1569, 1497, 1447 (s, sh, ν C=C_{arom} + ν C–H bend), 1349 (m, sh, ν CH_2), 1253 (m, sh, ν Ph-O), 1155 (s, sh, HCC, HCN bending, Im), 846, 761, 662. ^{1}H NMR (200 MHz, $CDCl_3$) δ (ppm): 13.48 (br, s, 2H, Ph-O**H**) 9.53 (s, 2H, N(1)C**H**N(3)- Im), 8.42 (s, 2H, 2× **H**–C=N), 7.80–7.77 (d, 2H, J_{HH} = 1.96 Hz, 2× N(1)CHC**H**-Im), 7.50–7.48 (d, J_{HH} = 2.12 Hz, 2H, 2× N(1)C**H**CH-Im), 7.36–7.29 (m, 4H, 4× Ph-**H**), 6.98–6.93 (m, 2H, 2× Ph-**H**), 5.36 (s, 4H, 2× –N(3)–C$\mathbf{H_2}$–Ph), 4.02–3.93 (q, 4H, 2× –N(1)C$\mathbf{H_2}$), 3.84–3.75 (m, 2H, 2× Cyhex-**H**), 1.85–1.42 (m, 8H, 8× Cyhex-**H**), 1.28–1.25 (t, J_{HH} = 6.99, 7.01 Hz, 6H, 2× –CH_2C$\mathbf{H_3}$). MALDI-TOF MS, *m/z*: 669.3 [M·H_2O + K]$^+$ and 573.3 [M – Cl]$^+$. Anal. Calcd. for $C_{32}H_{40}Cl_2N_6O_2$·H_2O (*M* = 629.62): C, 61.04; H, 6.72; N, 13.35; Found: C, 60.73; H, 6.33; N, 13.20. Conductivity = 265 μS/cm.

*2.2.4.3. N,N′-Bis[5-((1-n-butylidazolium)methylene)-salicylidene)-trans-1,2-cyclohexane-diamine dichloride (**4c**).* Pale yellow powder, (2.19 g, 77%). FT-IR (KBr, cm^{-1}): 3398 (m, br, ν O–H), 3140 (w, br, ν_{asym} CH, CH, Im and Ph), 3022 (m, br, ν_{sym} CH, Im and Ph), 2959 (m, sh, ν CH_3), 2888 (m, sh, ν CH_2), 1629 (vs, sh, ν C=N), 1573, 1487, 1438 (s, sh, ν C=C_{arom} + ν C–H bend), 1346 (m, sh, ν CH_2), 1260 (m, sh, ν Ph-O), 1158 (s, sh, HCC, HCN bending, Im), 843, 679, 561. ^{1}H NMR (200 MHz, $CDCl_3$) δ (ppm): 13.35 (br, s, 2H, 2× Ph-O**H**) 9.63 (s, 2H, 2× N(1) C**H**N(3)- Im), 8.28 (s, 2H, 2× **H**–C=N), 7.76–7.73 (d, 2H, J_{HH} = 1.87 Hz, 2× N(1)CHC**H**-Im), 7.65–7.63 (d, J_{HH} = 1.89 Hz, 2H, 2× N(1)C**H**CH-Im), 7.18–6.96 (m, 6H, 6× Ph-**H**), 5.34 (s, 4H, 2× –N(3)–C$\mathbf{H_2}$–Ph), 4.24–4.17 (t, J_{HH} = 7.08, 7.09 Hz, 4H, 2× –N(1)C$\mathbf{H_2}$), 4.00–

3.95 (m, 2H, 2× Cyhex-**H**), 1.92–1.76 (m, 8H, 8× Cyhex-**H**), 1.65–1.57 ($m_{(5)}$, 4H, 2× $-N(1)CH_2C\mathbf{H_2}$), 1.29–1.19 ($m_{(6)}$, 4H, 2× $-C\mathbf{H_2}CH_3$), 0.98–0.90 (t, J_{HH} = 7.05, 7.14 Hz, 6H, 2× $-CH_2C\mathbf{H_3}$). MALDI-TOF MS, *m/z*: 750.5 $[M{\cdot}2.5H_2O + K]^+$ and 631.3 $[M - Cl]^+$. Anal. Calcd. for $C_{36}H_{48}Cl_2N_6O_2{\cdot}2.5H_2O$ (*M* = 712.75): C, 60.66; H, 7.50; N, 10.02; Found: C, 60.62; H, 7.35; N, 9.60. Conductivity = 239 μS/cm.

*2.2.4.4. N,N′-Bis[3-tert-butyl-5-((2-methylimidazolium)methylene)-salicylidene)-trans-1,2-cyclo-hexandiamine dichloride (**4d**).* Canary yellow solid, (2.17 g, 76%). FT-IR (KBr, cm^{-1}): 3430 (m, br, ν O–H), 3295 (m, br, ν N(1)–H), 3086 (w, br, ν_{asym} CH, CH, Im and Ph), 2997 (m, br, ν_{sym} CH, Im and Ph), 2943 (m, sh, ν CH_3), 2868 (m, sh, ν CH_2), 1629 (vs, sh, ν C=N), 1593, 1476, 1443 (s, sh, ν C=C_{arom} + ν C–H bend), 1360 (m, sh, ν CH_2), 1281 (m, sh, ν Ph-O), 1149 (s, sh, HCC, HCN bending, Im), 897, 868, 775, 700, 655, 510. ^1H NMR (200 MHz, $CDCl_3$) δ (ppm): 13.75 (br, s, 2H, 2× Ph-O**H**) 10.05 (s, 2H, 2× N–**H** Im), 8.28 (s, 2H, 2× **H**–C=N), 7.65–7.64 (d, 2H, J_{HH} = 1.93 Hz, 2× N(1)CHC**H-** Im), 7.41–7.39 (d, J_{HH} = 1.99 Hz, 2H, 2× N(1)C**H**CH**-** Im), 7.16–6.99 (m, 4H, 4× Ph-**H**), 5.32 (s, 4H, 2× $-N(3)-C\mathbf{H_2}-Ph$), 3.60–3.56 (m, 2H, 2× Cyhex-**H**), 2.93 (s, 6H, 2× $C(2)-C\mathbf{H_3}$), 1.83–1.45 (m, 8H, 8× Cyhex-**H**), 1.22 (s, 18H, 2× $C(C\mathbf{H_3})_3$). MALDI-TOF MS, *m/z*: 736.5 $[M{\cdot}H_2O + Na]^+$ and 578.1 $[M{\cdot}H_2O-Cl]^+$. Anal. Calcd. for $C_{38}H_{52}Cl_2N_6O_2{\cdot}H_2O$ (*M* = 713.78): C, 63.94; H, 7.63; N, 11.77; Found: C, 64.12; H, 7.56; N, 11.48. Conductivity = 258 μS/cm.

*2.2.4.5. N,N′-Bis[3-tert-butyl-5-((1-ethylimidazolium)methylene)-salicylidene)-trans-1,2-cyclohexane-diamine dichloride (**4e**).* Pale yellow-orange powder, (2.00 g, 69%). FT-IR (KBr, cm^{-1}): 3446 (m, br, ν O–H), 3090 (w, br, ν_{asym} CH, CH, Im and Ph), 3005 (m, br, ν_{sym} CH, Im and Ph), 2954 (m, sh, ν CH_3), 2865 (m, sh, ν CH_2), 1634 (vs, sh, ν C=N), 1591, 1479, 1439 (s, sh, ν C=C_{arom} + ν C–H bend), 1362 (m, sh, ν CH_2), 1285 (m, sh, ν Ph-O), 1138 (s, sh, HCC, HCN bending, Im), 939, 828, 772, 711, 644. ^1H NMR (200 MHz, $CDCl_3$) δ (ppm): 13.68 (br, s, 2H, 2× Ph-O**H**) 10.03 (s, 2H, 2× N(1)C**H**N(3)-Im), 8.42 (s, 2H, 2× **H**–C=N), 7.58–7.56 (d, 2H, J_{HH} = 1.93 Hz, 2× N(1)CHC**H-** Im), 7.39–7.37 (d, J_{HH} = 1.99 Hz, 2H, 2× N(1)C**H**CH**-** Im), 7.26–6.98 (m, 4H, 4× Ph-**H**), 5.22 (s, 4H, 2× $-N(3)-C\mathbf{H_2}$-Ph), 4.58–4.53 (q, 4H, 2× $N(1)C\mathbf{H_2}$), 3.55–3.49 (m, 2H, 2× Cyhex-**H**), 1.89–1.44 (m, 8H, 8× Cyhex-**H**), 1.39 (s, 18H, 2× $C(C\mathbf{H_3})_3$), 1.24–1.20 (t, J_{HH} = 7.28, 7.30 Hz, 6H, 2× $-CH_2C\mathbf{H_3}$). MALDI-TOF MS, *m/z*: 671.4 $[M{\cdot}H_2O-2Cl]^+$. Anal. Calcd. for $C_{40}H_{56}Cl_2N_6O_2{\cdot}H_2O$ (*M* = 741.83): C, 64.76; H, 7.88; N, 11.33; Found: C, 64.45; H, 7.83; N, 11.00. Conductivity = 239 μS/cm.

*2.2.4.6. N,N′-Bis[3-tert-butyl-5-((1-butylimidazolium)methylene)-salicylidene)-trans-1,2-cyclohexane-diamine dichloride (**4f**).* Yellow-orange solid, (2.07 g, 65%). FT-IR (KBr, cm^{-1}): 3486 (m, br, ν O–H), 3055 (w, br, ν_{asym} CH, CH, Im and Ph), 2999 (m, br, ν_{sym} CH, Im and Ph), 2948 (m, sh, ν CH_3), 2880 (m, sh, ν CH_2), 1635 (vs, sh, ν C=N), 1560, 1478, 1444 (s, sh, ν C=C_{arom} + ν C–H bend), 1366 (m, sh, ν CH_2), 1284 (m, sh, ν Ph-O), 1176 (s, sh, HCC, HCN bending, Im), 1284 (m, sh, ν Ph-O), 851, 772, 646. ^1H NMR (200 MHz, $CDCl_3$) δ (ppm): 13.73 (br, s, 2H, 2× Ph-O**H**) 9.99 (s, 2H, 2× N(1)C**H**N(3)- Im), 8.68 (s, 2H, 2× **H**–C=N), 7.60–7.59 (d, 2H, J_{HH} = 1.90 Hz, 2× N(1)CHC**H-** Im), 7.41–7.39 (d, J_{HH} = 1.89 Hz, 2H, 2× N(1)C**H**CH**-** Im), 7.26–7.00 (m, 4H, 4× Ph-**H**), 5.28 (s, 4H, 2× $-N(3)-C\mathbf{H_2}$-Ph), 4.32–4.29 (t, J_{HH} = 6.99, 7.01 Hz, 4H, 2× $-N(1)C\mathbf{H_2}$), 3.48–3.43 (m, 2H, 2× Cyhex-**H**), 1.92–1.70 (m, 8H, 8× Cyhex-**H**), 1.63–1.55 ($m_{(5)}$, 4H, 2× $-N(1)CH_2C\mathbf{H_2}$), 1.36 (s, 18H, 2× $C(C\mathbf{H_3})_3$), 1.28–1.19 ($m_{(6)}$, 4H, 2× $-C\mathbf{H_2}CH_3$), 1.00–0.96 (t, J_{HH} = 7.12, 7.12 Hz, 6H, 2× $-CH_2C\mathbf{H_3}$). MALDI-TOF MS, *m/z*: 762.2 $[M{\cdot}H_2O-Cl]^+$. Anal. Calcd. for $C_{44}H_{64}Cl_2N_6O_2{\cdot}H_2O$ (*M* = 797.94): C, 66.23; H, 8.34; N, 10.53; Found: C, 66.30; H, 8.33; N, 10.10. Conductivity = 220 μS/cm.

*2.2.5. General procedure for the preparation of metallosaldach–imidazolium systems [M(III)Cl{$(R^1)_2$saldach($Im^+-R^2R^3-Cl^-)_2$}] (M = Mn, Fe) (**5**, **6a–f**)*

*2.2.5.1. Synthesis of Mn(III) complexes (**5a–f**).* A yellow solution of the substituted imidazolium-saldach ligand $H_2(R^1)_2$saldach($Im^+-R^2R^3-Cl^-)_2$ **4a–f** (0.9 mmol) in ethanol (10 mL) was degassed for 15 min. An ethanolic solution (5 mL) of $Mn(OAc)_2{\cdot}4H_2O$ (269 mg, 1.1 mmol) was then added with the yellow solution turning dark brown immediately, and the reaction mixture was refluxed for 2 h under N_2. LiCl (69.9 mg, 1.65 mmol) was then added and the solution was refluxed for an additional 2 h with air bubbled through the solution. After evaporating the solvent under reduced pressure, the residue was re-dissolved in CH_2Cl_2 (3 ml), over-layered with ethyl acetate (3 ml) and the mixture kept in a refrigerator overnight. The precipitated solid was filtered off and washed with ethyl acetate and diethyl ether. Recrystallization from CH_2Cl_2/n-hexane yielded pure [Mn(III)Cl{$(R^1)_2$saldach($Im^+-R^2R^3-Cl^-)_2$}] **5a–f**.

Chlorido-trans-[[2,2′-][(1,2-cyclohexanediyl) bis(nitrilo-methylidyne)] bis[4-((2-methylimidazolium)methylene-phenolato]-[N,N′,O,O′] manganese(III) dichloride (**5a**): Dark-brown powder (556 mg, 92%). FT-IR (KBr, cm^{-1}): 3286 (m, br, ν N(1)-H), 3133 (w, br, ν_{asym} CH, CH, Im and Ph), 2934 (m, sh, ν CH_3), 2859 (m, sh, ν CH_2), 1618 (vs, sh, ν C=N), 1559, 1472, 1436 (s, sh, ν C=C_{arom} + ν C–H bend), 1348 (m, sh, ν CH_2), 1275 (m, sh, ν Ph-O), 1167 (s, sh, ν HCC + ν HCN bending, Im), 826 (m, sh, ν Mn–N). MALDI-TOF MS, *m/z*: 710.9 $[M + K]^+$. Anal. Calcd. for $C_{30}H_{34}Cl_3MnN_6O_2$ (*M* = 671.93): C, 53.63; H, 5.10; N, 12.51; Found: C, 53.92; H, 5.02; N, 12.29. Conductivity = 351 μS/cm; μ_{eff} = 4.97 μ_B.

Chlorido-trans-[[2,2′-][(1,2-cyclohexanediyl) bis(nitrilo-methylidyne)] bis[4-((1-ethylimidazolium)methylene-phenolato]-[N,N′,O,O′] manganese(III) dichloride monohydrate (**5b**·H_2O): Brown powder (575 mg, 89%). FT-IR (KBr, cm^{-1}): FT-IR (KBr, cm^{-1}): 3426 (s, br, ν O–H H_2O), 3134 (w, br, ν_{asym} CH, CH, Im and Ph), 3078 (m, br, ν_{sym} CH, Im and Ph), 2934 (m, sh, ν CH_3), 2858 (m, sh, ν CH_2), 1621 (vs, sh, ν C=N), 1558, 1439 (s, sh, ν C=C_{arom} + ν C–H bend), 1346 (m, sh, ν CH_2), 1273 (m, sh, ν Ph-O), 1152 (s, sh, HCC, HCN bending, Im), 821 (m, sh, ν Mn–N), 471 (m, sh, ν Mn–O). MALDI-TOF MS, *m/z*: 722.3 $[M + Na]^+$. Anal. Calcd. for $C_{32}H_{38}Cl_2MnN_6O_2{\cdot}H_2O$ (Mw = 718.00): C, 53.53; H, 5.62; N, 11.70; Found: C, 53.83; H, 5.41; N, 11.68. Conductivity = 335 μS/cm; μ_{eff} = 4.95 μ_B.

Chlorido-trans-[[2,2′-][(1,2-cyclohexanediyl) bis(nitrilo-methylidyne)] bis[4-((1-butylimidazolium)methylene-phenolato]-[N,N′,O,O′] manganese(III) dichloride monohydrate (**5c**·H_2O): Reddish-brown powder (599 mg, 86%). FT-IR (KBr, cm^{-1}): 3436 (m, br, ν O–H H_2O), 3129 (w, br, ν_{asym} CH, CH, Im and Ph), 2935 (m, sh, ν CH_3), 2859 (m, sh, ν CH_2), 1614 (vs, sh, ν C=N), 1547, 1500, 1446 (s, sh, ν C=C_{arom} + ν C–H bend), 1347 (m, sh, ν CH_2), 1272 (m, sh, ν Ph-O), 1152 (s, sh, HCC, HCN bending, Im), 826 (m, sh, ν Mn–N), 468 (m, sh, ν Mn–O). MALDI-TOF MS, *m/z*: 796.8 $[M{\cdot}H_2O + Na]^+$. Anal. Calcd. for $C_{36}H_{46}Cl_3MnN_6O_3{\cdot}H_2O$ (*M* = 774.10): C, 55.86; H, 6.25; N, 10.86; Found: C, 56.01; H, 6.26; N, 10.84. Conductivity = 307 μS/cm; μ_{eff} = 4.96 μ_B.

Chlorido-trans-[[2,2′-][(1,2-cyclohexanediyl) bis(nitrilo-methylidyne)] bis[4-((2-methylimidazolium)methylene)-6-(t-Bu-phenolato]-[N,N′,O,O′] manganese(III) dichloride monohydrate (**5d**·H_2O): Brown solid (657 mg, 91%). FT-IR (KBr, cm^{-1}): 3411 (m, br, ν O–H H_2O), 3294 (m, br, ν N(1)–H), 2995 (w, br, ν_{asym} CH, CH, Im and Ph), 2941 (m, sh, ν CH_3), 2860 (m, sh, ν CH_2), 1616 (vs, sh, ν C=N), 1560, 1475, 1442 (s, sh, ν C=C_{arom} + ν C–H bend), 1356 (m, sh, ν CH_2), 1295 (m, sh, ν Ph-O), 1142 (s, sh, ν HCC + ν HCN bending, Im), 820 (m, sh, ν Mn–N), 465(m, sh, ν Mn–O). MALDI-TOF MS, *m/z*: 824.9 $[M{\cdot}H_2O + Na]^+$. Anal. Calcd. for $C_{38}H_{50}Cl_3MnN_6O_2{\cdot}H_2O$ (*M* = 802.15): C, 56.90; H, 6.53; N, 10.48; Found: C, 57.10; H, 6.43; N, 10.30. Conductivity = 327 μS/cm; μ_{eff} = 4.89 μ_B.

Chlorido-trans-[[2,2′-][(1,2-cyclohexanediyl) bis(nitrilomethylidyne)] bis[4-((1-ethylimidazolium)methylene)-6-(t-Bu-phenolato]-[N,N′,O,O′] manganese(III) dichloride monohydrate (**5e**·H_2O): Greenish-brown solid (672 mg, 90%). FT-IR (KBr, cm^{-1}): 3388 (m, br, ν O–H H_2O), 2997 (w, br, ν_{asym} CH, CH, Im and Ph), 2953 (m, sh, ν CH_3), 2860 (m, sh, ν CH_2), 1622 (vs, sh, ν C=N), 1585, 1475, 1440 (s, sh, ν C=C_{arom} + ν C–H bend), 1361 (m, sh, ν CH_2), 1298 (m, sh, ν Ph-O), 1136 (s, sh, ν HCC + ν HCN bending, Im), 819 (m, sh, ν Mn–N), 463(m, sh, ν Mn–O). MALDI-TOF MS, *m/z*: 830.6 $[M{\cdot}H_2O + H]^+$. Anal. Calcd. for $C_{40}H_{54}Cl_3MnN_6O_2{\cdot}H_2O$ (M = 830.21): C, 57.87; H, 6.80; N, 10.12; Found: C, 58.09; H, 6.76; N, 10.12. Conductivity = 307 μS/cm; μ_{eff} = 4.87 μ_B.

Chlorido-trans-[[2,2′-][(1,2-cyclohexanediyl) bis(nitrilomethylidyne)] bis[4-((1-butylimidazolium)methylene)-6-(t-Bu-phenolato]-[N,N′,O,O′] manganese(III) dichloride (**5f**): Faint-brown solid (680 mg, 87%). FT-IR (KBr, cm^{-1}): 3000 (w, br, ν CH, Im and Ph), 2947 (m, sh, ν CH_3), 2877 (m, sh, ν CH_2), 1623 (vs, sh, ν C=N), 1558, 1475, 1441 (s, sh, ν C=C_{arom} + ν C–H bend), 1360 (m, sh, ν CH_2), 1293 (m, sh, ν Ph-O), 1178 (s, sh, ν HCC + ν HCN bending, Im), 825 (m, sh, ν Mn–N), 468 (m, sh, ν Mn–O). MALDI-TOF MS, *m/z*: 832.3 $[M - Cl]^+$. Anal. Calcd. for $C_{44}H_{62}Cl_3MnN_6O_2$ (Mw = 868.30): C, 60.86; H, 7.20; N, 9.68; Found: C, 60.66; H, 7.24; N, 9.55. Conductivity = 291 μS/cm; μ_{eff} = 4.86 μ_B.

*2.2.5.2. Synthesis of Fe(III) complexes (**6a–f**).* A yellow solution of the substituted imidazolium-saldach ligand $H_2(R^1)_2$saldach(Im^+–R^2R^3–$Cl^-)_2$ **4a–f** (0.9 mmol) in ethanol (10 mL) was degassed for 15 min. An ethanolic solution (5 mL) of $FeCl_3{\cdot}6H_2O$ (178 mg, 1.1 mmol) was then added with the yellow solution turning dark reddish-brown immediately, and the reaction mixture was refluxed for 2 h under N_2. Then, the solution was concentrated and the residue was kept in a refrigerator overnight. The precipitated solid was filtered off and washed with cold ethanol (2 × 3 mL) and diethyl ether (3 × 3 mL) to yield [Fe(III)Cl{$(R^1)_2$saldach(Im^+–R^2R^3–$Cl^-)_2$}] **6a–f**.

Chlorido-trans-[[2,2′-][(1,2-cyclohexanediyl) bis(nitrilomethylidyne)] bis[4-((2-methylimidazolium)methylene)-phenolato]-[N,N′,O,O′] iron(III) dichloride dihydrate (**6a**·$2H_2O$): Reddish-brown powder (548, mg, 86%). FT-IR (KBr, cm^{-1}): 3408 (m, br, ν N(1)-H + ν O–H H_2O), 3154 (w, br, ν_{asym} CH, CH, Im and Ph), 2933 (m, sh, ν CH_3), 2862 (m, sh, ν CH_2), 1617 (vs, sh, ν C=N), 1559, 1441 (s, sh, ν C=C_{arom} + ν C–H bend), 1349 (m, sh, ν CH_2), 1279 (m, sh, ν Ph-O), 1166 (s, sh, ν HCC + ν HCN bending, Im), 817 (m, sh, ν Fe–N). MALDI-TOF MS, *m/z*: 709.2 $[M{\cdot}2H_2O + H]^+$. Anal. Calcd. for $C_{30}H_{34}FeN_6O_2{\cdot}2H_2O$ (M = 708.86): C, 50.83; H, 5.40; N, 11.86; Found: C, 51.24; H, 5.20; N, 11.48. Conductivity = 349 μS/cm; μ_{eff} = 5.84 μ_B.

Chlorido-trans-[[2,2′-][(1,2-cyclohexanediyl) bis(nitrilomethylidyne)] bis[4-((1-ethylimidazolium)methylene)-phenolato]-[N,N′,O,O′] iron(III) dichloride dihydrate (**6b**·$2H_2O$): Brown powder (484 mg, 73%). FT-IR (KBr, cm^{-1}): FT-IR (KBr, cm^{-1}): 3433 (s, br, ν O–H H_2O), 3136 (w, br, ν_{asym} CH, CH, Im and Ph), 3068 (m, br, ν_{sym} CH, Im and Ph), 2935 (m, sh, ν CH_3), 2861 (m, sh, ν CH_2), 1622 (vs, sh, ν C=N), 1559, 1507, 1443 (s, sh, ν C=C_{arom} + ν C–H bend), 1347 (m, sh, ν CH_2), 1271 (m, sh, ν Ph-O), 1152 (s, sh, HCC, HCN bending, Im), 832 (m, sh, ν Fe–N), 468 (m, sh, ν Fe–O). MALDI-TOF MS, *m/z*: 758.2 [M·$2H_2O$ + Na]. Anal. Calcd. for $C_{32}H_{38}Cl_3FeN_6O_2{\cdot}2H_2O$ (M = 736.92): C, 52.16; H, 5.74; N, 11.40; Found: C, 52.26; H, 5.53; N, 11.11. Conductivity = 331 μS/cm; μ_{eff} = 5.80 μ_B.

Chlorido-trans-[[2,2′-][(1,2-cyclohexanediyl) bis(nitrilomethylidyne)] bis[4-((1-butylimidazolium)methylene)-phenolato]-[N,N′,O,O′] iron(III) dichloride dihydrate (**6c**·~$2H_2O$): Dark-red powder (507 mg, 71%). FT-IR (KBr, cm^{-1}): 3432 (m, br, ν O–H H_2O), 3132 (w, br, ν_{asym} CH, CH, Im and Ph), 2933 (m, sh, ν CH_3), 2861 (m, sh, ν CH_2), 1616 (vs, sh, ν C=N), 1545, 1504, 1447 (s, sh, ν C=C_{arom} + ν C–H bend), 1350 (m, sh, ν CH_2), 1270 (m, sh, ν Ph-O), 1154 (s, sh, HCC, HCN bending, Im), 822 (m, sh, ν Fe–N), 463 (m, sh, ν Fe–O). MALDI-TOF MS, *m/z*: 821.5 [M.~$2H_2O$ + Na]$^+$. Anal. Calcd. for $C_{36}H_{46}Cl_3N_6O_2{\cdot}$ ~$2H_2O$ (M = 793.02): C, 54.52; H, 6.36; N, 10.60; Found: C, 54.11; H, 6.41; N, 10.51. Conductivity = 303 μS/cm; μ_{eff} = 5.78 μ_B.

Chlorido-trans-[[2,2′-][(1,2-cyclohexanediyl) bis(nitrilomethylidyne)] bis[4-((2-methylimidazolium)methylene)-6-(t-Bu-phenolato]-[N,N′,O,O′] iron(III) dichloride dihydrate (**6d**·$2H_2O$): Dark-red solid (584 mg, 79%). FT-IR (KBr, cm^{-1}): 3387 (m, br, ν O–H H_2O), 3293 (m, br, ν N(1)–H), 2995 (w, br, ν_{asym} CH, CH, Im and Ph), 2941 (m, sh, ν CH_3), 2860 (m, sh, ν CH_2), 1619 (vs, sh, ν C=N), 1567, 1478, 1443 (s, sh, ν C=C_{arom} + ν C–H bend), 1358 (m, sh, ν CH_2), 1291 (m, sh, ν Ph-O), 1145 (s, sh, ν HCC + ν HCN bending, Im), 801 (m, sh, ν Fe–N), 442 (m, sh, ν Fe–O). MALDI-TOF MS, *m/z*: 821.7 $[M{\cdot}2H_2O + H]^+$. Anal. Calcd. for $C_{38}H_{50}Cl_3FeN_6O_2{\cdot}2H_2O$ (M = 821.08): C, 55.59; H, 6.63; N, 10.24; Found: C, 56.00; H, 6.71; N, 9.88. Conductivity = 323 μS/cm; μ_{eff} = 5.76 μ_B.

Chlorido-trans-[[2,2′-][(1,2-cyclohexanediyl) bis(nitrilomethylidyne)] bis[4-((1-ethylimidazolium)methylene)-6-(t-Bu-phenolato]-[N,N′,O,O′] iron(III) dichloride dihydrate (**6e**·$2H_2O$): Dark-red solid (588 mg, 77%). FT-IR (KBr, cm^{-1}): 3389 (m, br, ν O–H H_2O), 3280 (m, br, ν N(1)–H), 2998 (w, br, ν_{asym} CH, CH, Im and Ph), 2953 (m, sh, ν CH_3), 2865 (m, sh, ν CH_2), 1617 (vs, sh, ν C=N), 1566, 1476, 1445 (s, sh, ν C=C_{arom} + ν C–H bend), 1357 (m, sh, ν CH_2), 1296 (m, sh, ν Ph-O), 1144 (s, sh, ν HCC + ν HCN bending, Im), 800 (m, sh, ν Fe–N), 438 (m, sh, ν Fe–O). MALDI-TOF MS, *m/z*: 887.6 $[M{\cdot}2H_2O + K]^+$. Anal. Calcd. for $C_{40}H_{54}Cl_3FeN_6O_2{\cdot}2H_2O$ (M = 849.13): C, 56.58; H, 6.88; N, 9.90; Found: C, 56.56; H, 6.87; N, 9.70. Conductivity = 305 μS/cm; μ_{eff} = 5.74 μ_B.

Chlorido-trans-[[2,2′-][(1,2-cyclohexanediyl) bis(nitrilomethylidyne)] bis[4-((1-butylimidazolium)methylene)-6-(t-Bu-phenolato]-[N,N′,O,O′] iron(III) dichloride monohydrate (**6f**·H_2O): Dark-red solid, (562 mg, 69%). FT-IR (KBr, cm^{-1}): 3432 (m, br, ν O–H H_2O), 2997 (w, br, ν CH, Im and Ph), 2948 (m, sh, ν CH_3), 2875 (m, sh, ν CH_2), 1625 (vs, sh, ν C=N), 1559, 1476, 1443 (s, sh, ν C=C_{arom} + ν C–H bend), 1361 (m, sh, ν CH_2), 1291 (m, sh, ν Ph-O), 1179 (s, sh, ν HCC + ν HCN bending, Im), 799 (m, sh, ν Fe–N), 436 (m, sh, ν Fe–O). MALDI-TOF MS, *m/z*: 909.9 [M·H_2O + Na]$^+$. Anal. Calcd. for $C_{44}H_{62}Cl_3FeN_6O_2{\cdot}H_2O$ (Mw = 887.22): C, 59.56; H, 7.27; N, 9.47; Found: C, 59.77; H, 7.65; N, 9.21. Conductivity = 288 μS/cm; μ_{eff} = 5.68 μ_B.

2.3. Antimicrobial activity

The plate-hole diffusion method was employed for the determination of antimicrobial activities against the gram (+), gram (−) bacterial and fungal organisms. Broth micro-dilution method was used to determine the MICs (minimum inhibitory concentrations) for the free ligands and their complexes in H_2O against test organisms. All tests were performed in duplicate and repeated twice. Modal values were selected. Each microorganism was seeded in tube with nutrient broth (NB) (1 cm^3) which was then homogenized in the tubes with 9 cm^3 of melted (45 °C) nutrient Agar (NA). The homogeneous suspensions were poured into Petri dishes and holes of 4 mm diameter were done in the cool medium. After cooling these holes, 100 μL of the investigated compounds solutions, with serial concentrations, were applied using a micropipette with the pathogens to be tested against. The plates were incubated for 72 h at 37 °C for bacteria and 28 °C for fungi, after that the clear zone around the wells was measured as inhibition zones and the diameter of these zone of inhibition (mm) were measured accurately. The antibacterial activities were observed and measured using a transparent meter rule and recorded if the zone of inhibition was ≥10 mm [25]. Ampicillin, Antibacterial, and Amphotericin B, Antifungal, were employed as standard drugs.

3. Results and discussion

3.1. Chemistry

3.1.1. Ligands synthesis

The syntheses of the six ligands **4a**–**f** is depicted in Scheme 2. The required starting materials salicylaldehyde-imidazolium chloride salts **2a**,**b** were synthesized starting from 2-substituted phenol following modified literature procedures [22,23,26]. Under extra dry conditions and using anhydrous magnesium dichloride as O-magnesiation reagent, 2-*tert*-butylphenol was formylated selectively ortho to the hydroxy group by paraformaldehyde with triethylamine as base. The substituted salicylaldehydes **1a**,**b** were then one-pot chloromethylated by reaction with paraformaldehyde and 37% HCl under a stream of HCl_g in the presence of a catalytic amount of $ZnCl_2$ or tetrabutylammonium bromide at room temperature to yield 5-chloromethylated salicylaldehydes **2a**,**b** in high purity. Modifying the R^1-group from hydrogen to a bulky t-butyl group increases the reaction time for chloromethylation at the 5-position from 1 to 3 days. Subsequent quarternization of alkylimidazole with **2a**,**b** generate salicylaldehyde-imidazolium chloride salts **3a**–**f**, which are the key intermediates in the synthesis of the achiral ligands. The chelating salts, (*rac-trans*-$H_2(R^1)_2$saldach(Im^+-R^2R^3-$Cl^-)_2$) **4a-f**, containing the saldach skeleton were synthesized through the Schiff-base condensation reaction of compounds **3a**–**f** with (±)-*trans*-1,2-diaminocyclohexane (*rac-trans* dach) in methanolic solution. The *rac-trans* configuration of *N*,*N*′-bis(salicylidene)-1,2-cyclohexanediamine (saldach) backbone was chosen, because it forces the ligand into a flat chair (planar) conformation similar to the 1,2-cyclohexanediamine moiety present in oxaliplatin, a very promising metal-based drug [27]. Ligands were isolated in high yields, gave satisfactory elemental analysis, and were characterized by spectroscopic techniques: ^{1}H NMR, ^{13}C NMR, FTIR, MALDI-TOF and conductivity measurements.

3.1.2. Synthesis of the metallosaldach–imidazolium chlorides

Mn(III)-saldach–imidazolium chlorides, synthesized by reaction of free ligands $H_2(R^1)_2$saldach(Im^+–R^2R^3–$Cl^-)_2$ (**4a**–**f**) and manganese(II) acetate tetrahydrate in 1 : 1 M ratio in UV-methanol in a Schlenk line under nitrogen atmosphere followed by aerobic oxidation in the presence of LiCl, are dark brown glassy solids. Fe(III) complexes **6a**–**f** were obtained by the reaction of equimolar free saldach ligands with iron(III) chloride hexahydrate under anaerobic conditions (Scheme 3). All synthesized compounds are soluble in water and most organic solvents. The resulting chelate complexes are highly soluble in common organic solvents and were fully characterized using elemental analyses and spectroscopic techniques FTIR, UV–Vis, MALDI-TOF, ESI-MS as well as conductivity and magnetic measurements.

Unfortunately, all attempts to obtain X-ray diffraction quality single crystals of the Mn(III)- and Fe(III)-saldach-imidazolium chlorides ((**5**,**6**)**a**–**f**) were unsuccessful. Nevertheless, the metal-ligand structures suggested in this work (based upon elemental and spectral analysis) match with the structures of reported metal-saldach analogs (Table S1, Supporting information).

3.2. Characterization of free ligands and their complexes

The molar conductance values of the ligands and their complexes ranging from 220 to 284 and 288–351 μS/cm, respectively, reveal their electrolytic nature.

3.2.1. ^{1}H NMR studies

The most remarkable feature of the ^{1}H NMR spectra for all ligands is the down-field singlet at 13.75–13.30 ppm which is assigned to the resonance of phenol OH [28,29]. The N–H of the imidazolium moiety in **4a**,**d** appears as a singlet at 9.48 and 10.05 respectively. The signal for the azomethine (CH=N) proton is observed at δ 8.68–8.28 ppm. Also, all saldach-imidazolium salts have two sets of resonance signals located in the aromatic region of the NMR spectrum (7.58–6.84 and 7.79–7.38 ppm) assigned to phenyl and imidazole protons, respectively. The signal set in the high-field region (4.00–3.43 and 1.85–1.42 ppm) is ascribed to the aliphatic cyclohexyl protons. To the best of our knowledge, the central saldach backbone is in the *O*-protonated tautomeric form not in the *N*-protonated tautomeric form (cf. Scheme 1) [32].

3.2.2. FTIR spectra

The selected IR spectra of the Schiff bases and their metal complexes along with their tentative assignments are reported in

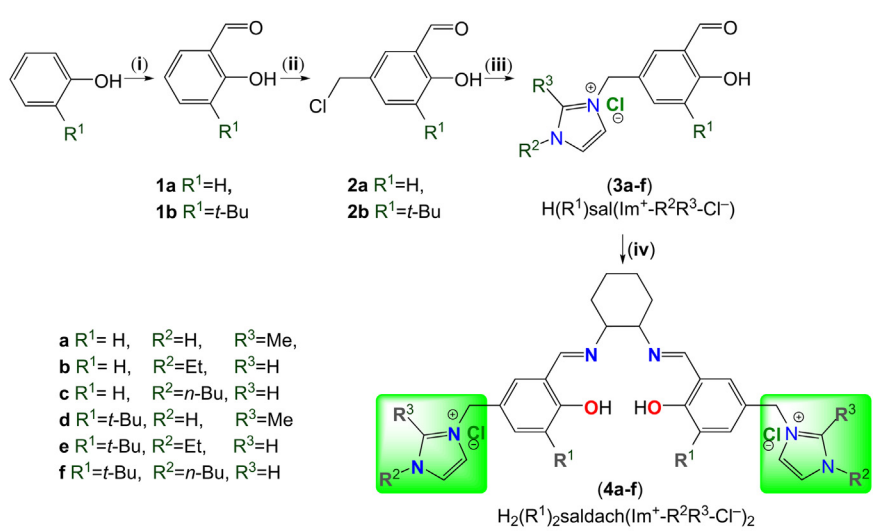

(**i**) 1. Anhydrous $MgCl_2$, $(CH_2O)_n$, Et_3N, ACN, stir, r.t; 2. HCl. (**ii**) CH_2O, $ZnCl_2$, HCl_{aq}, HCl_g, stir, r.t. (**iii**) Alkylimidazole, toluene, stir, 80 °C, N_2. (**iv**) MeOH, reflux, stir, N_2.

Scheme 2. Synthesis of salicylaldehyde- (**3a**–**f**) and saldach-imidazolium chloride salts, **4a**–**f**.

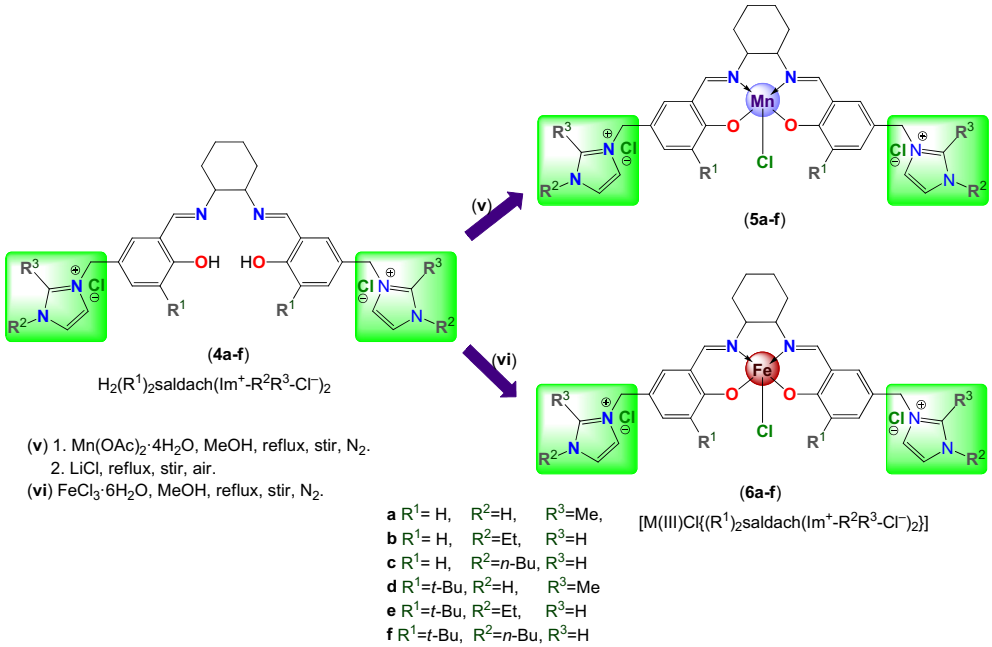

Scheme 3. Synthesis of Mn(III)- and Fe(III)-saldach–imidazolium chloride complexes, **5a–f 6a–f**, respectively.

Table S2 (Supporting information). In order to identify the IR signatures of the central saldach backbone, the bands caused by the terminal imidazolium compartments of saldach-imidazolium chloride have to be identified. The characteristic functionalities of saldach-imidazolium ligands include the hydrogen bonded hydroxyl groups, the azomethine groups (–C=N–) and the terminal imidazolium compartments. These functional groups were identified by comparing the spectroscopic data with literature values of similar systems. Broad peaks were observed around ~3400 cm^{-1} in their IR spectra which strongly suggested the presence of intramolecular hydrogen bonding OH group. Additionally, a band at 1280–1253 cm^{-1} was assigned to a mixed ν(Ar–O).

H_2saldach and H_2(2-^{t}Bu)$_2$saldach exhibit a C=N stretch at 1639 and 1641 cm^{-1}, respectively [30,31]. Introduction of an imidazolium group in (**4a–f**) results in a low-energy shift to 1635–1629 cm^{-1}. This low-energy shift of the azomethine band by introduction of imidazolium group reflects the C=N bond order reduction induced by the (–I) effect of quaternary N-atom and hydrogen bond with o-hydroxyl group [32]. The vibrational bands at ~846 and ~760 cm^{-1} should be assigned to the in-plane and out-of plane flexural vibration mode of the imidazolium ring respectively [33].

Formation of the complexes and their possible geometries were assigned on the basis of the electronic and infrared spectral studies, where in the absence of more powerful techniques such as X-ray, the FTIR data confirm its usefulness in the characterization of the coordination environments of these complexes ((**5**,**6**)**a–f**). So the study of the IR spectral data was quite informative in characterizing the metal-saldach binding modes.

All complexes exhibit very similar infrared spectral features. When comparing the spectroscopic data of Mn(III) and Fe(III) complexes with those of the free ligands, marked changes may be noticed in the ligand bands arising from various modes of donor groups involved in bonding to manganese and iron ions (Fig. 1). The diagnostic IR spectral bands with their assignments of the free ligands and their metal complexes are given in Table S1 (Supporting information). The IR stretching bands due to azomethine ν(HC=N) register a red-shift of 11–15 and 10–17 cm^{-1} in the manganese(III)- and iron(III)-saldach-imidazolium complexes, respectively (see Table 1), thus, indicating the coordination of the azomethine nitrogen to Mn(III) and Fe(III) ions [34], which is further confirmed by the appearance of a new band in the spectra of chelates at 543–570 cm^{-1} assigned to a νM(III)–N vibration (M = Mn, Fe) [35].

Strong bands attributable to phenolic oxygen ν(Ar–O) are evident; these all show a shift of 9–17 and 7–21 cm^{-1} to higher energy in the manganese(III)- and iron(III) complexes from the free ligand values indicative of co-ordination to Mn(III) and Fe(III) respectively [35a]. The new IR band (456–475 cm^{-1}) is assigned to M-O vibrations [35a,36] and supports the ligation of the phenolate oxygen to metal ions. Moreover the disappearance of the phenolic O–H vibration, originally found in the saldach-imidazolium salts, indicates that it is deprotonated in complexes.

The bands ascribed to the vibration of the imidazole ring remain unchanged in the Mn(III) and Fe(III) complexes revealing that, the nitrogen atom of the imidazole moiety does not take part in metal coordination [37]. Finally, very broad bands centered at ca. 3430

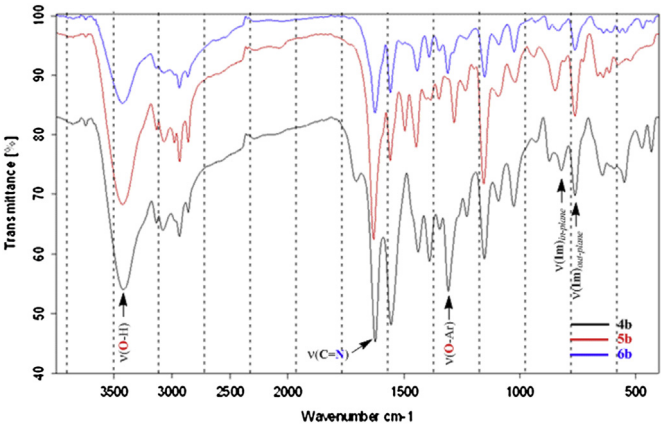

Fig. 1. Selected IR fragment, for comparing the azomethine and phenolate stretches and their splitting patterns from **4b**, **5b** and **6b**.

Table 1
Assignment of the vibrations that are responsible for the FTIR from the free saldach ligands (**4a**–**f**) and their complexes ((**5**,**6**)**a**–**f**).

Compound	ν HC=N	$\Delta\nu$ HC=N	ν O–H	ν Ar–O	$\Delta\nu$ Ar–O	ν Imidazole	ν M–N	ν M–O
4a	1630	–	3395	1258	–	761	–	–
5a	1618	−12	–	1275	+17	760	570	475
6a	1617	−13	3408	1279	+21	759	569	471
4b	1632	–	3434	1253	–	760	–	–
5b	1621	−11	3426	1273	+20	761	547	471
6b	1622	−10	3433	1271	+18	760	543	468
4c	1629	–	3398	1260	–	760	–	–
5c	1614	−15	3436	1272	+12	759	545	468
6c	1616	−13	3432	1270	+10	760	544	463
4d	1629	–	3430	1281	–	770	–	–
5d	1616	−13	3411	1295	+14	771	568	482
6d	1619	−10	3387	1291	+10	769	564	478
4e	1634	–	3446	1285	–	770	–	–
5e	1622	−12	3388	1298	+13	770	559	463
6e	1617	−17	3389	1296	+11	771	555	458
4f	1635	–	3486	1284	–	768	–	–
5f	1623	−12	–	1293	+9	769	565	468
6f	1625	−10	3432	1291	+7	768	562	456

and 3386 and 3424 cm^{-1} in some complexes can be assigned to the ν (OH) modes of lattice water in the corresponding framework [38].

These IR spectral studies reveal that the ligand coordinates to the metal ion in a tetradentate fashion through the deprotonated phenolate oxygen and azomethine nitrogen atoms (*i.e* with NONO (N_2O_2) donor sites).

3.2.3. *Electronic absorption spectroscopy and magnetic susceptibility*

The UV/Vis electronic spectra of the M(III)-saldach-imidazolium chloride complexes (M = Mn, Fe) (**5a**–**f**) (Table S3, Supporting information) exhibit similar features, where all display a shoulder and three intense absorption peaks at ranges (266–272, 306–311, 393–395, 500–508) and (258–263, 299–304, 381–384, 504–511) for Mn(III) and Fe(III) complexes, respectively, which are assigned to the intra- and inter-ligand charge transfer and d–d transition. The higher energy band (<300 nm) is due to intra-ligand $\pi \rightarrow \pi^*$ transitions ($\pi \rightarrow \pi^*$, LLCT), (phenyl and C=N moieties) [39]. Also higher energy bands (300–500 nm) are attributable to $n \rightarrow \pi^*$ (phenolic oxygen) intra-ligand transitions. The most important

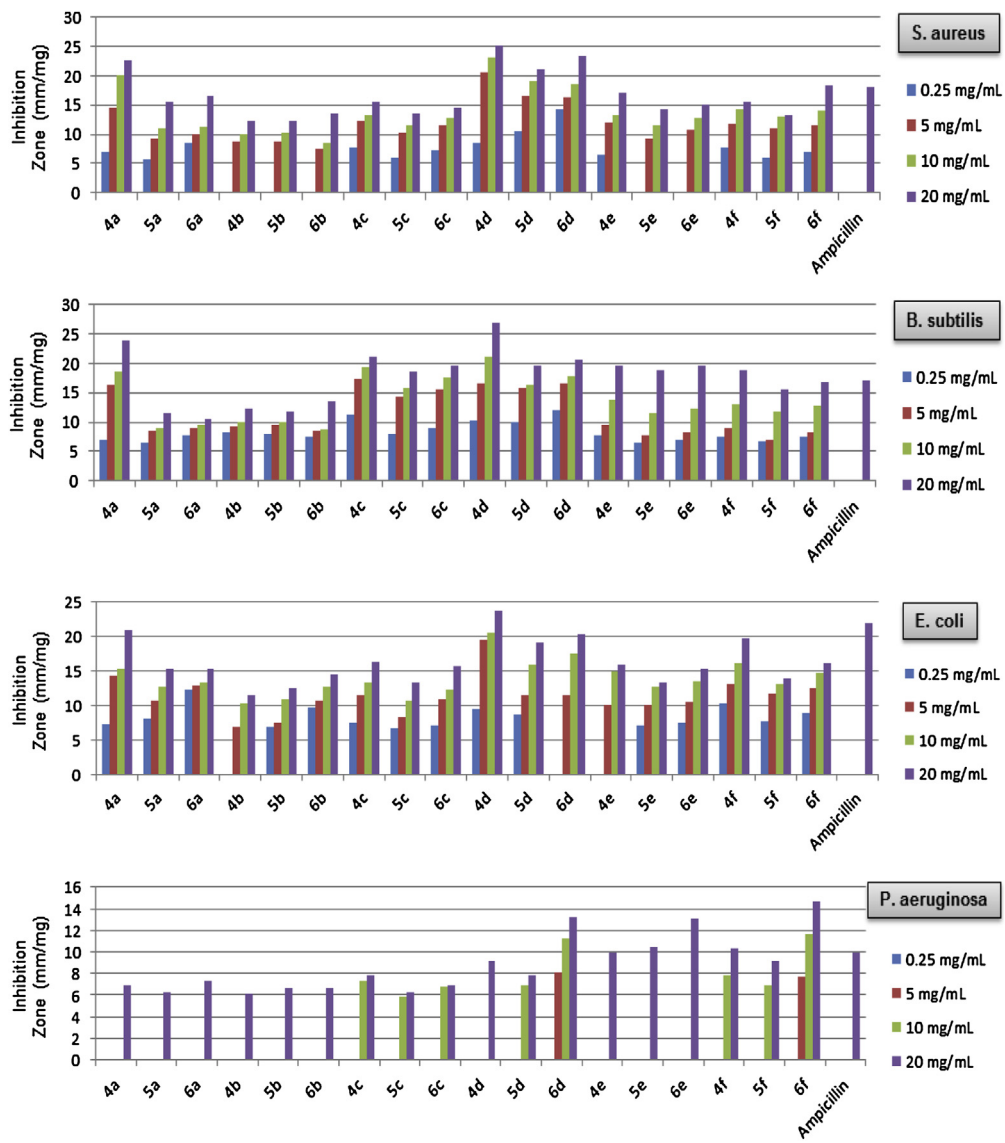

Fig. 2. Graph of zone of inhibition/mm for target compounds against different bacterial species.

feature in the near-UV region of the M(III)-saldach–imidazolium chloride is the higher wavelength band at (500–511 nm). These bands indicate the coordination of metal ion with the ligands, and this can be assigned to a charge-transfer band (MLCT), a transition from pπ orbitals on the phenolate oxygen atom to the dπ* orbitals of M(III) [40]. These bands in addition to a low intensity broad absorption bands (that may appear as shoulders > 600 nm) are assigned to the three allowed d–d transitions expected for complexes with a square pyramidal geometry, ($d_{xz} \rightarrow d_{x2-y2}$), ($d_{xy} \rightarrow d_{x2-y2}$, d_{yz}) and ($d_{z2} \rightarrow d_{x2-y2}$) [41]. The magnetic moment values for the complexes (4.86–4.97 μ_B for Mn(III) saldach and 5.68–5.84 μ_B Fe(III) saldach) are also supportive of square pyramidal geometry with high spin metal centers.

One can clearly observe the effect of the substitution of the H-atom in [M(III)Cl{(H)$_2$saldach(Im$^+$–R^{2}R^3–Cl$^-$)$_2$}] (M = Mn, Fe; (**5**,**6**)**a**–**c**) with the *tert*-butyl group [M(III)Cl{(^{t}Bu)$_2$saldach(Im$^+$–R^{2}R^3–Cl$^-$)$_2$}] (M = Mn, Fe; (**5**,**6**)**d**–**f**) upon UV absorption. The intensity of the two higher energy bands increased considerably as a result of enhancement the inter- and intra-ligand charge transfers. Also, the substitution shifts the absorption energy bands gradually to longer wavelengths. This effect is indicative of ligand π–$d\pi$ interactions between the saldach-imidazolium systems and the metal ion, which destabilize the ligand π molecular orbitals and decrease the π–π^* energy gap, thus producing a bathochromic shift.

3.3. Antimicrobial screening

3.3.1. Antibacterial activity

The free ligands (saldach-imidazolium chlorides, **4a**–**f**), their metal complexes (Mn(III)-saldach–imidazolium chlorides, **5a**–**f** and Fe(III)-saldach–imidazolium chlorides, **6a**–**f**) and the standard drug Ampicillin ($C_{16}H_{19}N_3O_4S$, 349.41 g mol^{-1}) were screened separately for their antibacterial activity against the bacteria *Staphylococus aureus* (*S. aureus*, ATCC-25923) and *Bacillus subtilis* (*B. subtilis*, Re-cultured) (as gram-positive bacteria) and Pseudomonas aeruginosa (*P. aeruginosa*, ATCC-27853) and *Escherichia coli* (*E. coli*, ATCC-25922) (as gram-negative bacteria) at 2.5, 5, 10 and 20 mg/mL concentrations. The diffusion agar technique was used to evaluate the antibacterial activity of the synthesized compounds [42]. As a parameter of antibacterial activity, the MIC values were determined from the percentages of inhibition at four different concentration levels. From the bactericidal activity data Table S4 (Supporting information), it has been observed that the ligand as well as its complexes show a significant degree of antibacterial activity against G$^+$ bacteria (*S. aureus*, *B. subtilis*) and *E. coli* from G$^-$ bacteria while slight activity or no activity toward *P. aeruginosa*. Generally it is apparent that all compounds were more toxic towards gram positive strains than gram negative strains. This could be ascribed to their cell-wall structural differences, where the walls of gram negative species are more complex than those of gram positive cells, so it might be difficult for the compounds to diffuse inside the G$^-$-bacterial cell. The zones of inhibition (ZOI) values are susceptible to the concentration of the compound used for inhibition (Fig. S1, Supporting information). The activity is greatly enhanced at the higher concentration. The ZOI values obtained indicate that the ligands have moderate to high activities as compared to Ampicillin drug towards the infection organisms (*S. aureus*, *B. subtilis*, *E. coli*). *N*,*N*′-Bis[3-*tert*-butyl-5-((2-methylimidazolium)methylene)-salicylidene)]-*trans*-1,2-cyclohexane-diamine dichloride (**4d**) and its Fe(III) complex (**6d**) exhibit remarkable extra-potent bactericidal activity (Fig. 2), higher than the standard drug. Moreover, their MIC values are quite small. The MIC values Table 2 for ligand (**4d**) against *S. aureus*, *B. subtilis* and *E. coli* were 14.88, 12.14, and 13.30 μg/mL while for complex (**6d**) assigned 8.74, 10.33, and >250 μg/mL and, thus, can be classified as a new good candidate in the fight against bacterial infections.

Nature of the cell wall, the ligand, coordination sites, geometry of the compound, the positive charge density, hydrophilicity, lipophilicity, presence of co-ligand, pharmacokinetic factors, etc. also play decisive roles in determining antimicrobial activity of the Schiff base and its metal complexes [43]. These factors may affect the fight against bacterial infections in two different ways: (i) interactions of compound with microbial cell wall, whereas the cationic charges on the imidazolium enhance the bactericidal activity, which is partially credited to the electrostatic attraction between the positively charged ligand or complex and negatively charged cells walls [43]. (ii) Ability of tested compound to penetrate cell walls by simply dissolving into and through the lipophilic cell wall, recent results indicate that hydrophobic groups may increase the antimicrobial activity [44]. The variation in the antimicrobial activity of different compounds against different microorganisms depends on their impermeability of the cell or the differences in ribosomes in microbial cell [45]. The lipid membrane surrounding the cell favors the passage of any lipid soluble materials and it is known that lipophilicity is an important factor controlling antimicrobial activity [46]. In the present study, low activity of the some metal complexes is due to their low lipophilicity, because of which penetration of the complex through the lipid membrane was decreased and hence, they could neither block nor inhibit the growth of the microorganism.

From the data it has been also observed that the activity depends upon the type of metal ion and varies in the following order of the metal ion: Fe > Mn.

3.3.2. Proposed mechanisms of bactericidal action

A major component of a bacterial cell wall is peptidoglycan, that is, polysaccharide chains of alternating N-acetylglucosamine (NAG)

Table 2
Minimum inhibitory concentration (MIC) profiles of the saldach-imidazolium chlorides and their M(III) complexes against different strains.

Sample	Minimum inhibitory concentration (MIC) (μg mL^{-1} sample)					
	Bacteria				Fungi	
	G$^+$ bacteria		G$^+$ bacteria			
	S. aureus	*B. subtilis*	*E. coli*	*P. aeruginosa*	*A. flavus*	*C. albicans*
4a	17.60	17.50	17.12	>10000	−ve	>250
5a	21.50	19.23	15.43	>10000	−ve	−ve
6a	14.85	16.03	**10.16**	>10000	−ve	>250
4b	>250	15.24	>250	>10000	−ve	>250
5b	>250	15.62	18.38	>10000	−ve	−ve
6b	>250	16.89	12.88	>10000	−ve	−ve
4c	16.23	11.16	16.66	>5000	−ve	>250
5c	21.18	15.41	18.65	>5000	−ve	−ve
6c	17.12	13.73	17.86	>5000	−ve	90.50
4d	14.88	12.14	13.30	>10000	−ve	**55.50**
5d	**11.90**	12.35	14.37	>5000	−ve	−ve
6d	**8.74**	**10.33**	>250	>250	−ve	>250
4e	18.39	16.03	>250	>10000	−ve	>250
5e	>250	19.23	17.60	>10000	−ve	>250
6e	>250	17.50	16.66	>10000	−ve	>250
4f	16.02	16.44	12.25	>5000	−ve	85.25
5f	21.18	18.38	16.23	>5000	−ve	−ve
6f	18.11	16.66	14.40	>250	−ve	>250
Ampicillin (Antibaterial drug)	**12.50**	**20.00**	**15.00**	**>1000**	−ve	−ve
Amphotericin B (Antifungal drug)	−ve	−ve	−ve	−ve	**40.00**	**80.00**

Bold values signify the most potent compounds in comparison with the tested standard drugs.

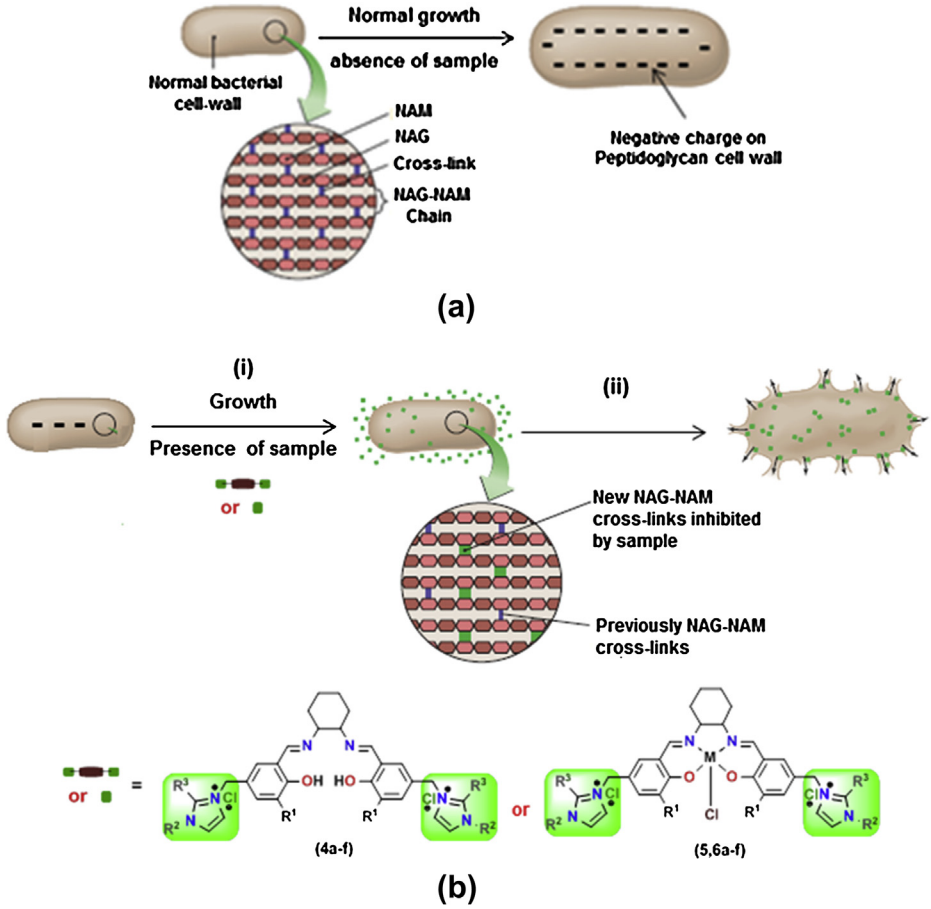

Fig. 3. Bacterial cell wall synthesis and the inhibitory effects of H_2saldach-Im chlorides and their complexes on it.

and N-acetylmuramic acid (NAM) molecules that are cross-linked by peptide bonds between NAM subunits [47].

There are no recent studies of the mechanisms of bactericidal action of Schiff bases. Earlier work had suggested that the bacterial cell wall was a major target site [43b], especially the major wall component peptidoglycan. Where the Schiff base and its complex indulge in the formation of hydrogen bonded interaction through the coordinated anion, hydroxyl group etc. with the active centers of the microbial cell constituents this results in interference with the normal cell processes.

Also saldach-imidazolium chlorides and their complexes may inhibit the peptidoglycan formation by irreversibly binding to the enzymes that cross-link NAM subunits and preventing the cross-linkage of NAM subunits (Fig. 3).

3.3.3. *Antifungal activity*

The free ligands (**4a**–**f**), M(III) complexes ((**5**,**6**)**a**–**f**) and standard antifungal drug (Amphotericin B, $C_{47}H_{73}NO_{17}$) were subjected for *in vitro* antifungal studies against *Aspergillus flavus* (*A. flavus*) *Candida albicans* (*C. albicans*, NCIM No. 3100) at 2.5, 5, 10 and 20 mg/mL concentration. From the experimental data Table S4 (Supporting information), all saldach-imidazolium chlorides and their Fe(III) salts exhibited moderate antifungal activity against *C. albicans* infection, and the ZOI values slight increase as the concentration of tested compound raised from 2.5 to 20 mg/mL. However, they could not inhibit the growth of the *A. flavus*. None of the Mn(III)-saldach–imidazolium chloride salts has shown any observable activity against each fungal species. All tested compounds are infective against fungal strains. These limited or lack of fungicidal activity could be attributed to two possibilities: (i) the complex structure of fungal cell-wall, composed typically of chitin, 1,3-β- and 1,6-β-glucan, mannan and proteins [48], which may reduce or completely stop tested compound to pass through in by diffusion. (ii) Fungal fighting proceeds by much more complex mechanisms than bacterial conflict. Compound (**4d**) was identified as the most active against *C. albicans*.

Acknowledgments

This work was in part supported by DFG grant Ja466/24-1 (initiation of bilateral cooperation RFME-CJ).

Appendix A. Supplementary data

Supplementary data related to this article can be found at http://dx.doi.org/10.1016/j.ejmech.2013.09.029.

References

[1] A. Tanitame, Y. Oyamada, K. Ofuji, M. Fujimoto, K. Suzuki, T. Ueda, H. Terauchi, M. Kawasaki, K. Nagai, M. Wachi, J. Yamagishi, Bioorg. Med. Chem. 12 (2004) 5515–5524.
[2] D.T. Chu, J.J. Plattner, L. Katz, J. Med. Chem. 39 (1996) 3853–3874.
[3] R.S. Levings, D. Lightfoot, S.R. Partridge, R.M. Hall, S.P. Djordjevic, J. Bacteriol. 187 (2005) 4401–4409.
[4] C. Schnellmann, V. Gerber, A. Rossano, V. Jaquier, Y. Panchaud, M.G. Doherr, A. Thomann, R. Straub, V. Perreten, J. Clin. Microbiol. 44 (2006) 4444–4454.
[5] J.R. Govan, V. Deretic, Microbiol. Rev. 60 (1996) 539–574.
[6] L. Ballell, R.A. Field, K. Duncan, R.J. Young, Antimicrob. Agents Chemother. 49 (2005) 2153–2163.

[7] J.F. Barrett, J.A. Hoch, Antimicrob. Agents Chemother. 42 (1998) 1529–1536.
[8] T. Miyamoto, J. Matsumoto, K. Chiba, H. Egawa, K. Shibamori, A. Minamida, Y. Nishimura, H. Okada, M. Kataoka, M. Fujita, T. Hirose, J. Nakano, J. Med. Chem. 33 (1990) 1645–1656.
[9] N. Nakada, H. Shimada, T. Hirata, Y. Aoki, T. Kamiyama, J. Watanabe, M. Arisawa, Biological characterization of cyclothialidine, Antimicrob. Agents Chemother. 37 (1993) 2656–2661.
[10] I. Correia, J.C. Pessoa, M. Teresa Duarte, M.F. Minas da Piedade, T. Jackush, T. Kiss, M.M.C.A. Castro, C.F.G.C. Geraldes, F. Avecilla, Eur. J. Inorg. Chem. (2005) 732–744.
[11] D. Barton, W.D. Ollis, Comprehensive Organic Chemistry, vol. 2, Pergamon, Oxford, 1979.
[12] (a) R.W. Layer, The chemistry of imines, Chem. Rev. 63 (1963) 489–510;
(b) H. Tanaka, A. Ağar, M. Yavuz, J. Mol. Model 16 (2010) 577–587.
[13] P.A. Vigato, S. Tamburini, Coord. Chem. Rev. 248 (2004) 1717–2128.
[14] B.M. Drašković, G.A. Bogdanović, M.A. Neelakantan, A.-C. Chamayou, S. Thalamuthu, Y.S. Avadhut, J. Schmedt auf der Günne, S. Banerjee, C. Janiak, Cryst. Growth Des. 10 (2010) 1665–1676.
[15] L. Shi, W.-J. Mao, Y. Yang, H.-L. Zhu, J. Coord. Chem. 62 (2009) 3471–3477.
[16] M.A. Phaniband, S.D. Dhumwad, Transition Met. Chem. 32 (2007) 1117–1125.
[17] G. Kumar, S. Devi, R. Johari, E-Journal of Chemistry 9 (2012) 2119–2127.
[18] F. Pfannkuch, H. Rettig, P.H. Stahl, C.G. Wermuth, P.H. Stahl, Handbook of Pharmaceutical Salts: Properties, Selection, and Use, Wiley-VCH, Weinheim, Germany, 2002, p. 130.
[19] (a) J. Pernak, K. Sobaszkiewicz, I. Mirska, Green Chem. 5 (2003) 52;
(b) J. Pernak, I. Goc, I. Mirska, Green Chem. 6 (2004) 323–329;
(c) M.T. Garcia, N. Gathergood, P.J. Scammells, Green Chem. 7 (2005) 9–14;
(d) P.J. Scammels, J.L. Scott, R.D. Singer, Aust. J. Chem. 58 (2005) 155–169;
(e) N. Gathergood, P.J. Scammels, Aust. J. Chem. 55 (2002) 557–560;
(f) J. Łuczak, C. Jungnickel, I. Łacka, S. Stolte, J. Hupka, Green Chem. 12 (2010) 593–601.
[20] S.V. Malhotra, V. Kumar, Bioorg. Med. Chem. Lett. 20 (2010) 581–585.
[21] (a) R.F. El-Shaarawy, Synthesis and Reactions of Some Pyridoyl Derivatives with Anticipated Biological Activities. M.Sc. thesis, Suez Canal University, Egypt, 2001;
(b) B. Wisser, C. Janiak, Z. Anorg. Allg. Chem. 633 (2007) 1796–1800;
(c) R.F. El-Shaarawy, H.K. Ibrahim, E. Eltamany, I. Mohy-Eldeen, Maced. J. Chem. Chem. Eng. 27 (2008) 65–79;
(d) A.-C. Chamayou, M.A. Neelakantan, S. Thalamuthu, C. Janiak, Inorg. Chim. Acta 365 (2011) 447–450;
(e) R.F.M. El-Shaarawy, C. Janiak, I.M. El-Deen, E.H. El-Tamany, J. Mol. Struct. (2013) (submitted, in review).
[22] G. Casiraghi, G. Casnati, M. Cornia, A. Pochini, G. Puglia, G. Sartori, R. Ungaro, J. Chem. Soc. Perkin Trans. 1 (1978) 318–321.
[23] Y. Yang, J.Q. Guan, P.P. Qiu, Q.B. Kan, Transition Met. Chem. 35 (2010) 263–270.
[24] L. Canali, E. Cowan, H. Deleuze, C.L. Gibson, D.C. Sherrington, J. Chem. Soc. Perkin Trans. 1 (2000) 2055–2066.
[25] A.J. Vlietink, L. Van Hoof, J. Totte, H. Laure, D.V. Berhe, P.C. Rwangabo, J. Mrukiyunmwami, J. Ethnopharmacol. 46 (1995) 31–47.
[26] P.U. Naik, G.J. McManus, M.J. Zaworotko, R.D. Singer, Dalton Trans. (2008) 4834–4836.
[27] A. Hille, I. Ott, A. Kitanovic, I. Kitanovic, H. Alborzinia, E. Lederer, S. Wölfl, N. Metzler-Nolte, S. Schäfer, W.S. Sheldrick, C. Bischof, U. Schatzschneider, R. Gust, J. Biol. Inorg. Chem. 14 (2009) 711–725.
[28] R.C. Felicio, E.T.G. Cavalheiro, E.R. Dockal, Polyhedron 20 (2001) 261–268.
[29] A. Clearfield, R. Gopal, R.J. Kline, M. Sipski, L.O. Urban, J. Coord. Chem. 7 (1978) 163–169.
[30] M.R. Mauryaa, A.K. Chandrakar, S. Chand, J. Mol. Catal. A 270 (2007) 225–235.
[31] P.J. Pospisil, D.H. Carsten, E.N. Jacobsen, Chem. Eur. J. 2 (1996) 974–980.
[32] C.-G.F. Richthofen, A. Stammler, H. Bögge, T. Glaser, J. Org. Chem. 77 (2012) 1435–1448.
[33] S. Tait, R.A. Osteryoung, Inorg. Chem. 23 (1984) 4352–4360.
[34] (a) F.X. Webster, R.M. Silverstein, Spectrophotometer Identification of Organic Compounds, sixth ed., 87,, John Wiley, New York, 1992;
(b) O. Pouralimardan, A.-C. Chamayou, C. Janiak, H.H. -Monfared, Inorg. Chim. Acta 360 (2007) 1599–1608;
(c) R.I. Kureshy, K.J. Prathap, T. Roy, N.C. Maity, N.H. Khan, S.H.R. Abdi, H.C. Bajaj, Adv. Synth. Catal. 352 (2010) 3053–3060;
(d) T. Chang, L. Jin, H. Jing, Chem. Cat Chem. 1 (2009) 379–383.
[35] (a) K. Nakomoto, Infrared and Raman Spectroscopy of Inorganic and Coordination Compounds, third ed., Wiley Interscience, New York, 1978;
(b) G. Karimipour, M. Montazerozohori, N.H. Naeini, Iran. J. Chem. Chem. Eng. 30 (2011) 13–18;
(c) X. Guojin, W. Saili, F. Yingguo, Z. Libo, T. Yuhai, Z. Yuansuo, Chin. J. Catal. 33 (2012) 473–477.
[36] G.B. Pethe, A.R. Yaul, J.B. Devhade, A.S. Aswar, Der Pharma Chem. 2 (2010) 301–308.
[37] J. Huang, X. Fu, G. Wang, Q. Miao, G. Wang, Dalton Trans. 41 (2012) 10661–10669.
[38] K. Nakamato, Infrared and Raman Spectra of Inorganic and Coordination Compounds, fourth ed., Wiley, New York, 1986, p. 242.
[39] A. Silva, C. Freire, B. de Castro, New J. Chem. 28 (2004) 253–260.
[40] L.J. Boucher, M.O. Farrell, J. Inorg. Nucl. Chem. 35 (1973) 3731–3738.
[41] B.P. Gaber, V. Miskowski, T.G. Spiro, J. Am. Chem. Soc. 96 (1974) 6868–6873.
[42] A. Rahman, M.I. Choudhary, W.J. Thomsen, Bioassay Techniques for Drug Development, Harwood Academic Publishers, The Netherlands, 2001, p. 16.
[43] (a) M. Kong, X.G. Chen, K. Xing, H.J. Park, Int. J. Food Microbiol. (2010) 51–63;
(b) V.P. Daniel, B. Murukan, B.S. Kumari, K. Mohanan, Spectrochim. Acta A: Mol. Biomol. Spectrosc. 70 (2008) 403–410.
[44] E.I. Rabea, M.E.I. Badawy, T.M. Rogge, C.V. Stevens, M. Höfte, W. Steurbaut, G. Smagghe, Pest Manage Sci. 61 (2005) 951–960.
[45] S.K. Sengupta, O.P. Pandey, B.K. Srivastava, V.K. Sharma, Transition Met. Chem. 23 (1998) 349–353.
[46] G. Kumar, D. Kumar, C.P. Singh, A. Kumar, V.B. Rana, J. Serb. Chem. Soc. 75 (2010) 629–637.
[47] S. Fujii, H. Kumagai, M. Noda, Carbohydr. Res. 83 (1980) 389–393.
[48] R.F. Hector, Clin. Microbiol. Rev. 6 (1993) 1–21.